



Synthesis of primary production in the Arctic Ocean: III. Nitrate and phosphate based estimates of net community production

L.A. Codispoti^{a,*}, V. Kelly^b, A. Thessen^c, P. Matrai^d, S. Suttles^e, V. Hill^f, M. Steele^g, B. Light^g

^a University of Maryland Center for Environmental Science, Horn Point Lab., P.O. Box 775, Cambridge, MD 21613-0775, USA

^b Green Eyes, LLC, 5745 Lovers Lane, Cambridge, MD 21613, USA

^c Marine Biology Lab., 7 MBL Street, Wood Hole, MA 02543, USA

^d Bigelow Laboratory for Ocean Sciences, 60 Bigelow Dr., E. Boothbay Harbor, ME 04544, USA

^e SES Consulting, 118 West End Ave., Cambridge, MD 21613, USA

^f Ocean, Earth and Atmospheric Sciences, Old Dominion University, 4600 Elkhorn Ave., Norfolk, VA 23529, USA

^g Applied Physics Laboratory, University of Washington, 1013 NE 40th Street, Seattle, WA 98105, USA

ARTICLE INFO

Article history:

Available online 20 December 2012

ABSTRACT

Combining nitrate, nitrite and phosphate data from several sources with additional quality control produced a database that eliminates many questionable values. This database, in turn, facilitated estimation of net community production (NCP) in the Arctic Marine System (AMS). In some regions, the new database enabled quantitative calculation of NCP over the vegetative season from changes in nutrient concentrations. In others, useful inferences were possible based on nutrient concentration patterns. This analysis demonstrates that it is possible to estimate NCP from seasonal changes in nutrients in many parts of the Arctic, however, the data were so sparse that most of our estimates for 14 sub-regions of the AMS are attended by uncertainties >50%. Nevertheless, the wide regional variation of NCP within the AMS (~two orders of magnitude) may make the results useful.

NCP for the entire AMS was estimated as 345 ± 72 Tg C over the vegetative season. Converting this value to annual primary production (PP) as determined by typical ^{14}C incubations suggests an annual primary production rate for the AMS of ~ 1000 Tg C.

We divided the AMS and its marginal seas into the same 13 sub-regions employed in the companion studies of Matrai et al. (2012) and Hill et al. (2013) and estimated NCP for each. We also made separate estimates for the Eurasian and Amerasian portions of the Arctic Basin.

Significant findings include:

1. NCP in the Arctic Basin is low, but there are regional variations in the controls and in rates. In the Amerasian Basin (particularly in the Canada sub-basin), nitrate concentrations from 0 to ~ 50 m are very low (~ 0 μM) even in winter. Thus, nutrient limitation suppresses NCP in this region. In the Eurasian Basin, light or grazing or both may be important limiting factors since significant surface layer nutrient concentrations persist during summer.
2. Low wintertime nitrate concentrations in the upper layers of the Amerasian Basin and Northern Beaufort Sea suggest that NCP in these sub-regions may be insensitive to changes in the ice and light regimes.
3. Although tentative because of limitations in the data, we group NCP in the 14 sub-regions as follows:
 - a. Very high NCP (~ 70 – 100 g C m^{-2}) in the Bering and Southern Chukchi sub-regions.
 - b. High NCP (~ 30 – 40 g C m^{-2}) in the Nordic and Barents seas and the Canadian Archipelago.
 - c. Moderate NCP (>10 to ~ 15 g C m^{-2}) in the Eurasian Basin, Southern Beaufort, Southern East Siberian Sea + Laptev, Kara Sea and Greenland Shelf sub-regions.
 - d. Low (NCP ~ 10 g C m^{-2}) in Northern East Siberian Sea + Laptev and Northern Chukchi sub-regions.
 - e. Extremely low NCP (~ 1 – 5 g C m^{-2}) in the Northern Beaufort and Amerasian Basin sub-regions.

© 2012 Elsevier Ltd. All rights reserved.

* Corresponding author.

E-mail addresses: codispot@hpl.umces.edu (L.A. Codispoti), vince@gescience.com (V. Kelly), athessen@eol.org (A. Thessen), pmatrai@bigelow.org (P. Matrai), steven.suttles@verizon.net (S. Suttles), vhill@odu.edu (V. Hill), mas@apl.washington.edu (M. Steele), bonnie@apl.washington.edu (B. Light).

1. Introduction

The Arctic Ocean (AO) and its marginal seas (Fig. 1a) are a highly heterogeneous, under-sampled marine system undergoing rapid change. With respect to primary production (PP), enough is known to assert that there are regional variations in the AMS that rival the PP range that can be found in the rest of the world ocean (e.g. Sambrotto et al., 1984; Stein and Macdonald, 2004; Sakshaug, 2004; Codispoti et al., 2005; Hill and Cota, 2005; Table 1).

Given the regional heterogeneity, the dramatic seasonal changes, the poor quality of much of the data, and limited access, obtaining a comprehensive picture of the AMS's primary productivity regime is difficult. Rapid climate change and inter-annual changes (e.g. Serreze et al., 2009; Tremblay and Gagnon, 2009) add additional difficulties. Nevertheless, there has been some progress during the past ~20 years. For example, we now suspect that early estimates of PP in the AMS were too low due to faults with methodology and a failure to account for early blooms of ice-algae and phytoplankton (e.g. Smith et al., 1991; Wheeler, 1997). In addition, some recent studies (e.g. Hill and Zimmerman, 2010; Hill et al., 2013) suggest that PP estimated from remotely sensed ocean color is too low in many cases because of underestimation of PP that occurs deeper than the ~1.2 optical depths accessible via satellite.

Decreasing snow/ice cover and ice thickness will cause the AMS to receive more photosynthetically active radiation (PAR) suggesting that there will be significant increases in PP. The trajectory for

Table 1
Annual primary production estimates selected from Sakshaug (2004).

| Region | Particulate primary production ($\text{g C m}^{-2} \text{ a}^{-1}$) | |
|--|---|-----------|
| | Total | New |
| Central Deep Arctic Ocean ^a | >11 | <1 |
| Arctic Shelf Seas (average) ^b | 32 | 8 |
| Beaufort Sea | 30–70 | 7–17 |
| Barents Sea | <20–200 | <8–100 |
| Bering Sea | >230 | – |
| Canadian Arctic | 20–40 | 5–10 |
| Chukchi Sea | 20 to >400 | 5 to >160 |
| Atlantic Sector (average) ^c | 97 | 50 |
| Baffin Bay | 60–120 | 25–50 |
| Greenland Sea | 70 | 40 |
| Norwegian Sea | 80–150 | 35–65 |
| Icelandic Sea | 100–200 | 45–90 |

^a Amerasian and Eurasian Basins.

^b Average for the Barents and its north slope, and the White, Kara, Laptev, East Siberian, Chukchi, Beaufort, and Lincoln Seas, the NE Water Polynya, and the North Water Polynya.

^c Average for Baffin Bay, Hudson Bay, Greenland Sea, Labrador Sea, Norwegian Sea and Icelandic Sea.

net community production (NCP) is less certain because of its dependency on a nutrient supply whose changes with warming are, at present, poorly constrained (e.g. Tremblay and Gagnon, 2009).

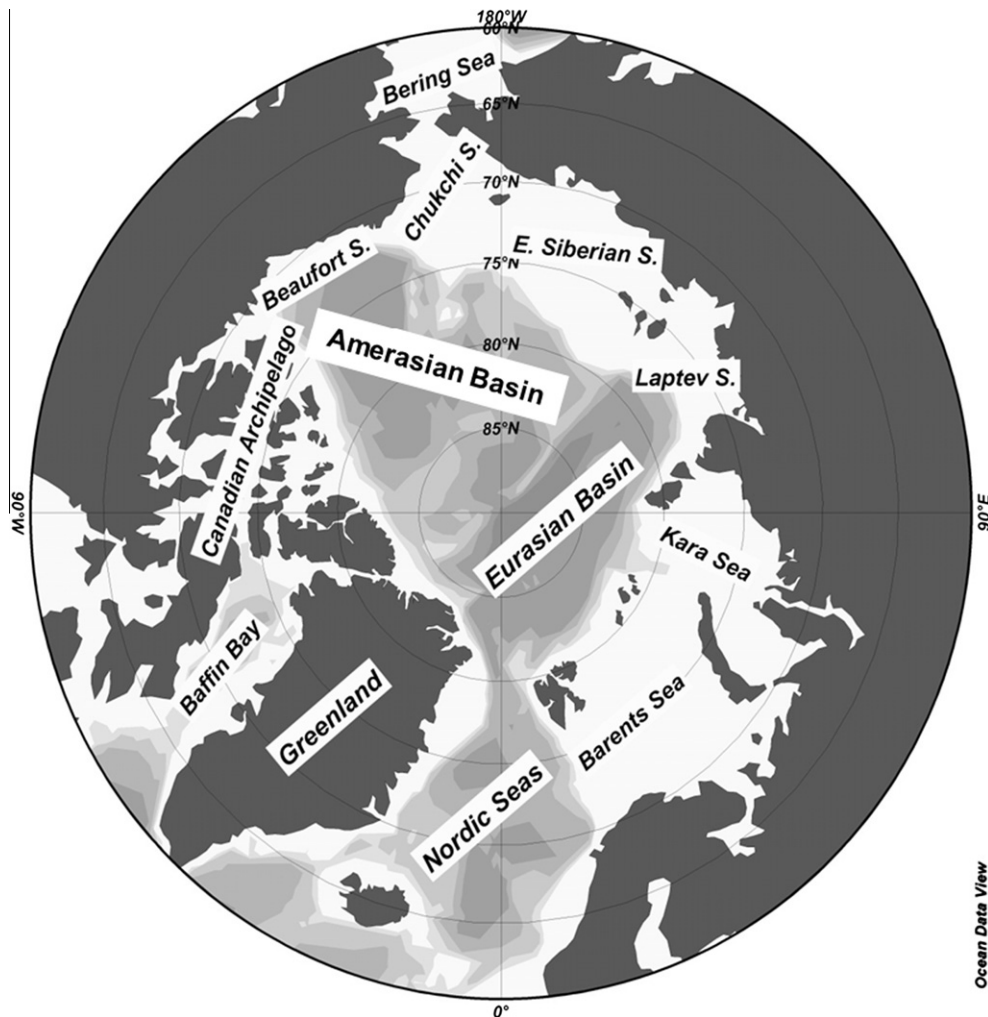


Fig. 1a. Location chart for the Arctic Ocean and its Marginal Seas.

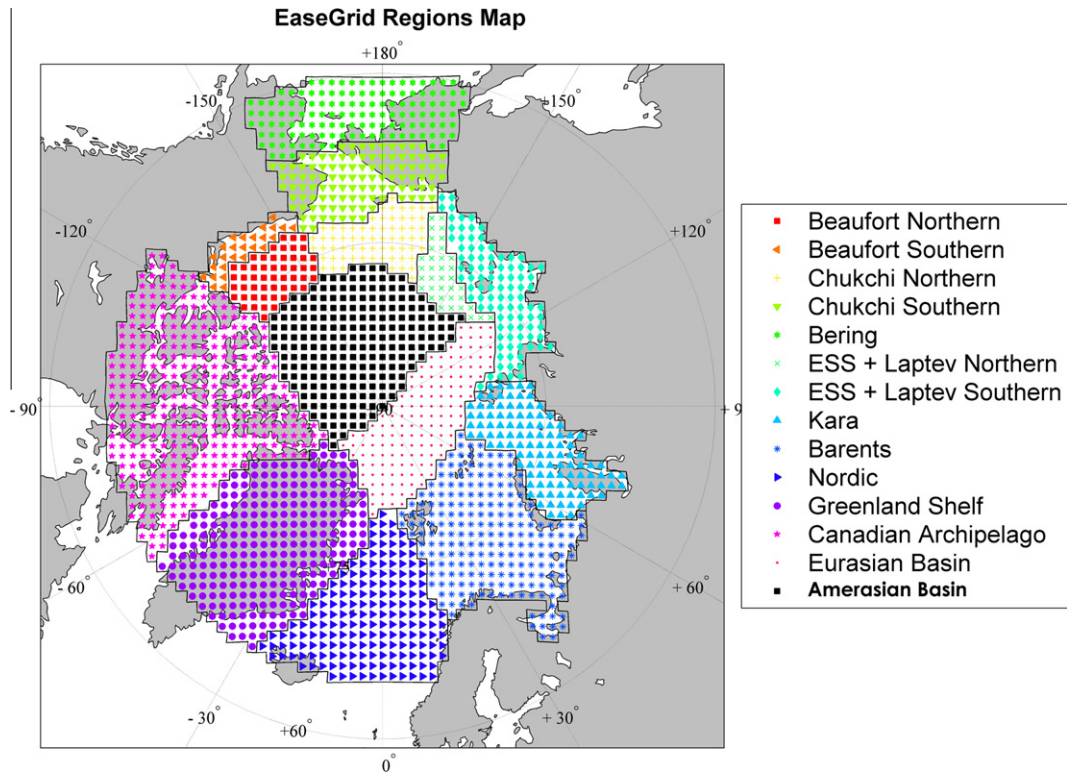


Fig. 1b. The EASE grid and its 14 sub-regions. In the companion papers of Matrai et al. (2012) and Hill et al. (2013), the Eurasian and Amerasian basins are combined into one Arctic Basin sub-region.

In this contribution, we examine pan-Arctic nitrate and phosphate distributions in order to estimate NCP. This component of biological production is more closely related to the AMS's ability to sequester carbon and to export material from the photic zone than is PP. We have produced NCP estimates for the 14 sub-regions shown in Fig. 1b and for the entire AMS. We have also converted these estimates of NCP into a total PP rate for the AMS by relying on the “*f*-ratio” concept (Eppley and Peterson, 1979; Le Bouteiller, 1993).

Note that, for brevity, a suite of Supplementary figures and tables that informed our analysis is omitted from this text. These are referred to as Tables S1–S3 and Figs. S1–S43 and are included as an addendum to this submission. These figures and tables are not essential for understanding this contribution, but they help substantiate its conclusions and provide background.

2. Scientific background

2.1. Controls on primary production

The major controls on aquatic PP and NCP are nutrient availability and radiation. These direct controls are, in turn, modulated by stratification and circulation features that enhance or constrain the nutrient supply and/or influence the radiation exposure of phytoplankton. These controls have interconnected feedbacks amongst themselves and also with the cryosphere and the atmosphere. The AMS combines these controls in distinctive ways. For example, with the exception of the Nordic Seas, the AMS is strongly salt-stratified, and circulation is relatively weak (Carmack, 2007). This salt stratification produces strong near-surface stratification and thin surface mixed layers. The nutrient regime is complex, in part because of significant differences in the Atlantic and Pacific inputs that lie on either end of the global conveyor belt (e.g. Berger, 1970; Broecker, 1991; Gordon, 1986; Fig. 2). In addition, nutrient concen-

trations in the water masses of Pacific origin differ significantly amongst themselves (Fig. 3). Internal processes such as the removal of fixed nitrogen by sedimentary denitrification significantly influence nutrient concentrations and ratios (e.g. Codispoti et al., 2009), and distinct signatures can be seen near river mouths.

The amount of radiation available for photosynthesis in the upper ocean is a function of the transmittance through the atmosphere and clouds, through the snow and ice cover, and finally, through the water column itself. Because NCP depends on the nutrient supply (e.g. Eppley and Peterson, 1979; Williams, 1993b) and because nitrate depletion is common (Figs. 4a–c) during the vegetative season, NCP in the AMS may be limited more by the nutrient supply than by light. Increased light penetration due to anticipated reductions in snow/ice cover may, however, increase NCP modestly. This is because increased light penetration could increase the utilization of nutrients present in shallow summertime nutriclines (e.g. Fig. S1). In addition, surface nitrate concentrations in the Eurasian Basin can be significant even during summer (Figs. 4c and S2). This condition could result from light limitation, or grazing pressure, or both (Olli et al., 2007). Reduced snow and ice cover might make this pool of nitrate more available to phytoplankton. As noted in Section 1, the impact of climate change on NCP in the AMS is poorly constrained because one can construct scenarios that increase or decrease the nutrient supply (e.g. Tremblay and Gagnon, 2009; Wassmann and Reigstad, 2011).

2.2. Stratification and buoyancy fluxes

Freshwater buoyancy fluxes are very large during summer on most AMS shelves due to ice melt, runoff, and the low salinity (particularly during summer) of the inflowing Pacific Waters (Carmack et al., 2006; Woodgate et al., 2006; Fig. 2). These processes create relatively shallow mixed layers that, via the general circulation, extend into the central basins. Summer mixed layers in the AMS are

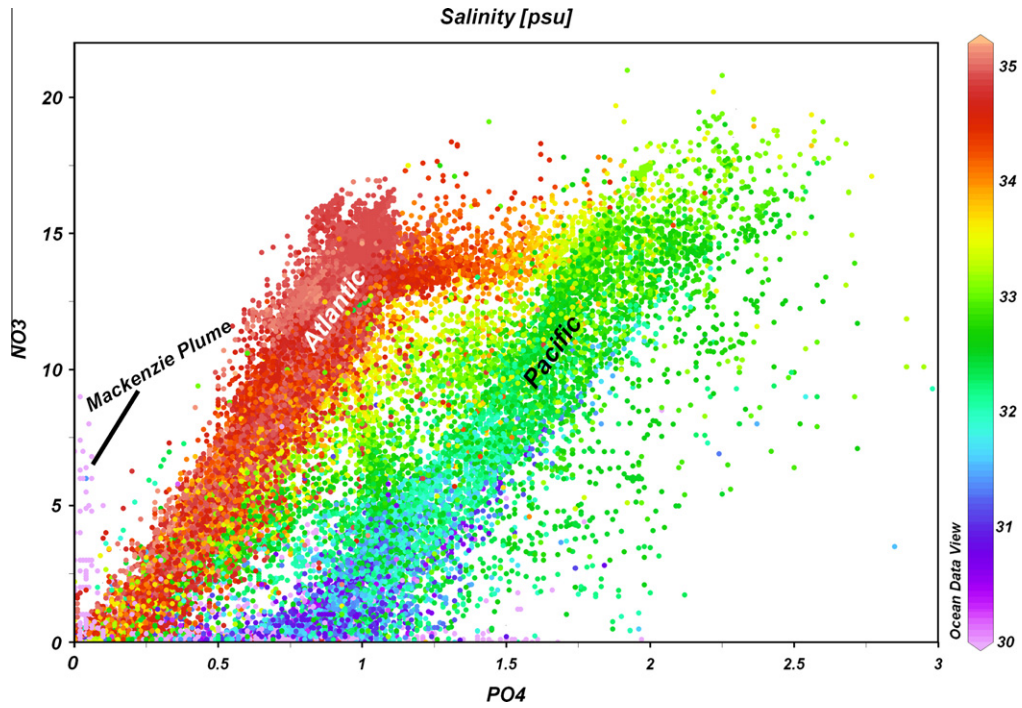


Fig. 2. Scatter diagram of nitrate vs. phosphate concentrations (in μM). Salinity is indicated by the color scale. The differences in phosphate values at ~ 0 nitrate show a clear difference between the higher salinity waters of Atlantic origin and the lower salinity waters of Pacific origin. Extremely low nitrate/phosphate ratios occur over the western Chukchi and eastern East Siberian Sea shelves. They are a signal of sedimentary denitrification.

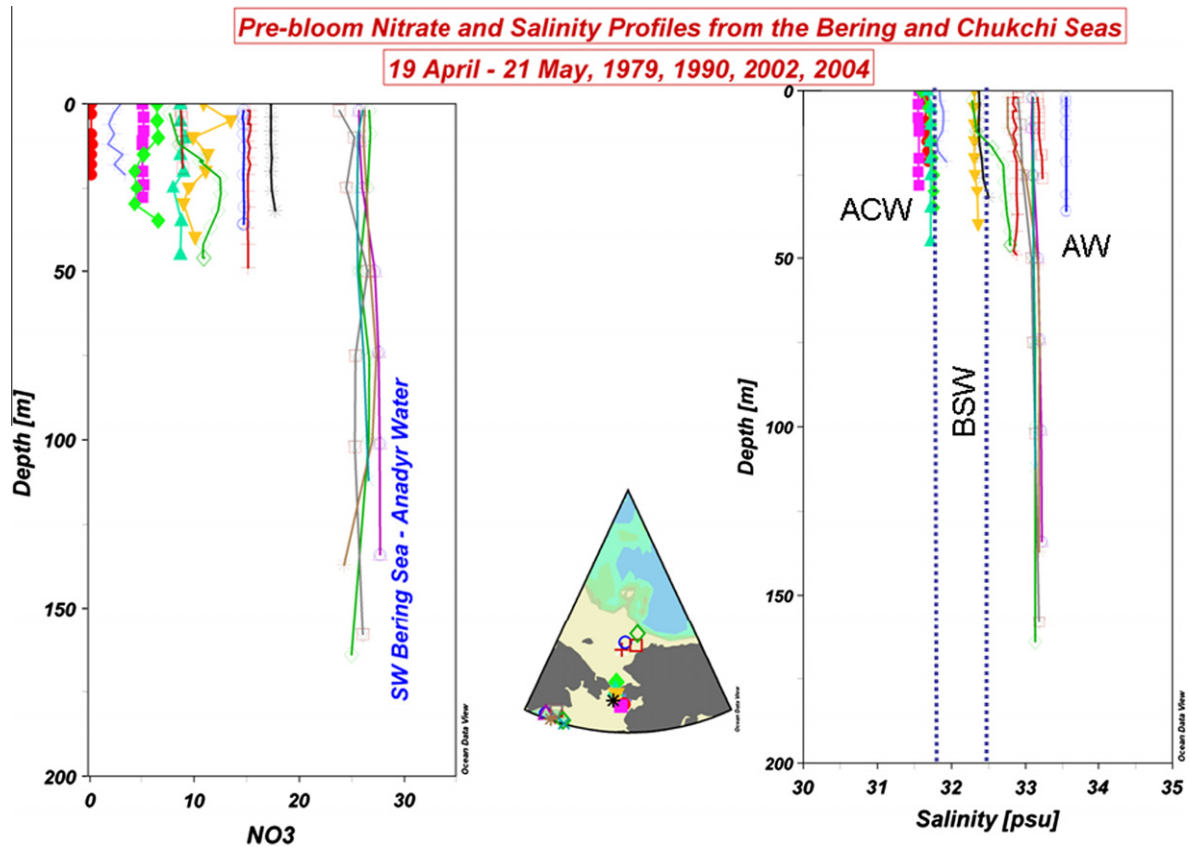


Fig. 3. Pre-bloom nitrate (in μM) and salinity profiles in the Bering and Chukchi Seas, that display significant differences in nutrient concentrations in the Pacific origin water masses that enter the Arctic. ACW = Alaskan Coastal Water. AW = Anadyr Water. BSW = Bering Shelf Water.

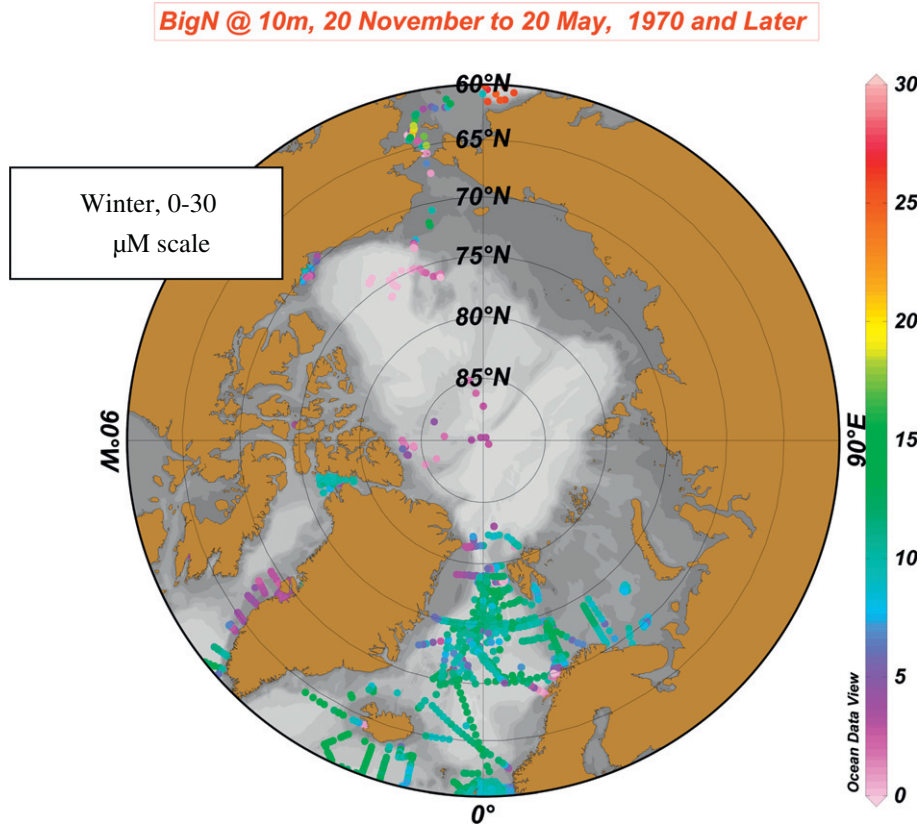


Fig. 4a. BigN (nitrate or nitrate + nitrite) concentrations in μM at 10 m during “winter” (20 November–20 May), color scale = 0–30 μM .

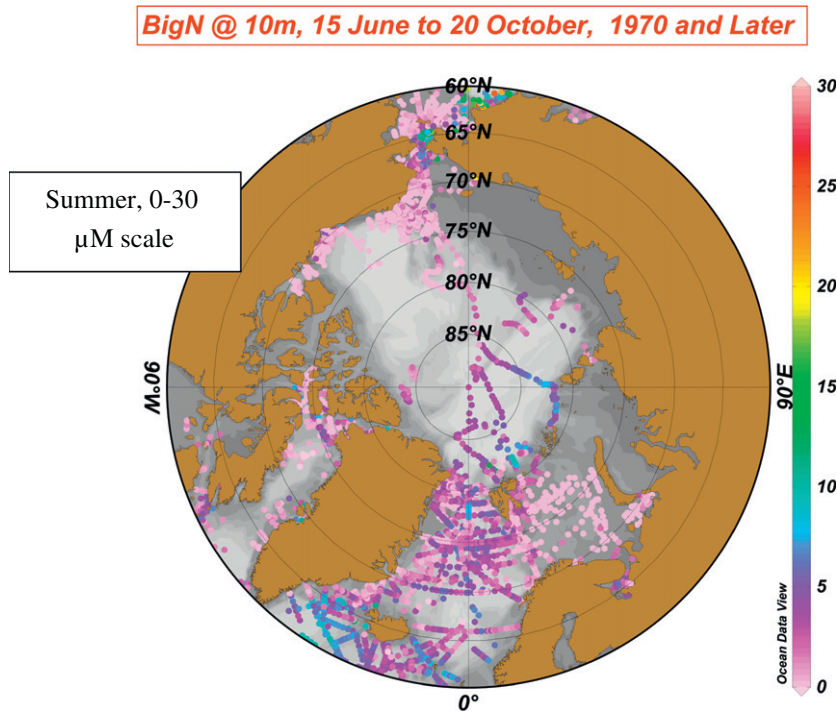


Fig. 4b. BigN (nitrate or nitrate + nitrite) concentrations in μM at 10 m during “summer” (15 June–20 October), color scale = 0–30 μM .

often <10 m deep (e.g. Codispoti et al., 2005), and throughout most of this system mixed layer depths seldom exceed 50 m even during winter (Carmack, 2007; Steele and Boyd, 1998). The strong stratification places an important constraint on the nutrient supply to

the AMS’s photic zone. The principal exceptions are the Nordic and Barents seas. In the Nordic Seas winter convection can extend to the abyss during deep water formation, and in both regions nutrient distributions suggest that the signals of seasonal

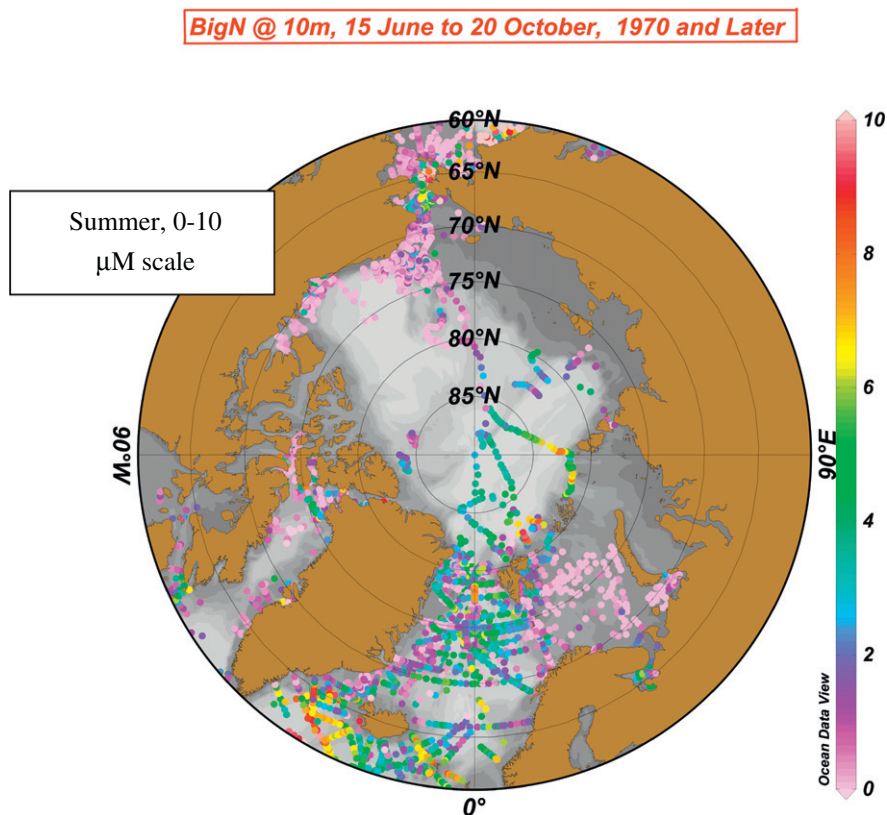


Fig. 4c. BigN (nitrate or nitrate + nitrite) concentrations in μM at 10 m during “summer” (15 June–20 October). Same as Fig. 4b except that the color scale = 0–10 μM to better indicate occurrences of nitrate depletion.

phytoplankton nutrient uptake can extend to depths of ~ 100 m (Codispoti et al., 1991; Figs. S3 and S4). With warming, buoyancy fluxes to the AMS are projected to increase due to increased river flows, increased erosion of ice-rich coastlines, and increased glacial melt (e.g. Jones et al., 2009; Peterson et al., 2002).

2.3. Mixing, upwelling and downwelling

Wind mixing events during the vegetative season increase PP, NCP and the vertical extent of the zone of seasonal nutrient uptake in the Nordic and Barents seas (Figs. S3 and S4). Sakshaug and Slagstad (1992) suggest that such events can significantly increase PP and new production in the Barents Sea. Tidal mixing is another factor that can introduce nutrients into the photic zone during the vegetative season. Stirling (1980) suggests that this process could be significant in the Canadian Archipelago. The same can be said for mesoscale eddies that by virtue of the vertical motions associated with them (e.g. Smith and Niebauer, 1993) can add nutrients to the photic zone. These processes extend the vertical extent of the zone of net nutrient uptake by transporting the signal of photic zone uptake downwards as they are transporting nutrients upwards.

Wind stress in the central Arctic is relatively weak, owing to the dominating Beaufort High (Zhang et al., 2000) and the damping effect of the sea ice pack. The Beaufort High induces downwelling and low photic zone nutrient concentrations in the Amerasian Basin (particularly the Canada sub-Basin). The associated upwelling on surrounding continental shelves (Aagaard, 1984) provides a nutrient source that may increase with warming (Carmack et al., 2006). Upwelling of nutrients is enhanced in canyons (Carmack et al., 2006; Pickart et al., 2009, 2011). Upwelling is also known to be important for stimulating PP in specific regions such as the North Water Polynya (Tremblay et al., 2002). Upwelling of Anadyr

Water (AW) maintains high nutrient concentrations in the vicinity of western Bering Strait year-round (Fig. S5).

The overall significance of upwelling in enhancing NCP is, however, poorly constrained. For example, upwelling occurs over the Beaufort Shelf mostly in fall and winter in association with the passage of some Aleutian Lows (Pickart et al., 2011). Thus, the immediate impact of upwelling on productivity may be reduced by low light levels. In addition upwelling during the vegetative season may have difficulty reaching the photic zone due to the strong salt stratification. The main impact of upwelling in regions like the Beaufort Sea may be to charge shelf waters with nutrients prior to the vegetative season (Carmack et al., 2006). Although the ice regime has an important impact on PP via its influence on radiation and stratification, ice-edge upwelling may not be important in supplying nutrients to the photic zone (Smith and Niebauer, 1993). The reduction of ice-cover could, however, increase the occurrence of wind-driven upwelling (Carmack et al., 2006).

2.4. Advective nutrient inputs

The largest nutrient inputs to the AMS are advective inputs via the Atlantic and Pacific entrances. The Atlantic and Pacific influenced regions of high productivity are, however, distinctly different. Although not so far apart on a global scale, the placement of the continents puts these inputs on different extremities of global circulation patterns for nutrients and water vapor (e.g. Berger, 1970; Broecker, 1991; Carmack, 2007; Gordon, 1986). Consequently, the Pacific input is less saline and richer in nutrients than the Atlantic input (Fig. 2). Although the total volume of Pacific Origin waters entering the Arctic is much less than the volume of the Atlantic inflow, the low salinity of the Pacific inflow (Fig. 2) concentrates its effect in the upper layers. As a consequence, the impact of the Pacific inflow rivals or exceeds the impact of the

Atlantic inflow with respect to nutrient inputs to the photic zone. These advective transports support the high PP and NCP found in the Nordic Seas and over the “inflow shelves” (*sensu* Carmack et al., 2006) of the Barents, Bering, Chukchi and eastern East Siberian seas.

The Atlantic approaches are deep, and throughout the water column nitrate:phosphate ratios are close to the atomic N:P Redfield Ratio of 15–16:1 (Redfield et al., 1963). Stratification is weak compared to the salt stratification found in the Pacific approaches. In the Nordic Seas (Fig. 1b), pre-bloom nutrient concentrations tend to be uniform with mean phosphate concentrations of $\sim 0.8 \mu\text{M}$ and mean nitrate concentrations of $\sim 11\text{--}12 \mu\text{M}$ (Fig. S3). Conditions in the Barents Sea are similar except that there may be a broader range of pre-bloom nitrate concentrations (Fig. S4). This uniformity in pre-bloom nutrient concentrations facilitates estimates of NCP based on seasonal changes in nitrate and phosphate concentrations.

Because of far-field and local denitrification, nitrate/phosphate ratios are generally less than 15–16:1 in the Pacific approaches to the Arctic and in the upper $\sim 100\text{--}150$ m of the portions of the AMS strongly influenced by Pacific waters (e.g. Codispoti and Richards, 1968; Codispoti et al., 2009; Fig. 2). As a consequence, NCP generally depletes nitrate in Pacific influenced waters before phosphate is exhausted. As already noted, the Pacific influenced regions also contain water masses with significantly different pre-bloom nutrient concentrations (Fig. 3). Highest photic zone nutrient concentrations occur in the Anadyr Water (AW) that enters the Bering Sea via the SW Bering Sea slope and thence the Arctic Ocean via western Bering Strait. In the AW maximum nitrate concentrations exceed $25 \mu\text{M}$ (Hansell et al., 1989; Fig. 3) and can be $>20 \mu\text{M}$ even during summer (Fig. S5). Maximum phosphate concentrations in the AW can exceed $2.5 \mu\text{M}$.

The year-round northerly flow of AW and topography (Stabeno et al., 2005) produce a persistent upwelling that maintains high nutrient concentrations in the northwestern Bering Sea, western Bering Strait and in adjacent portions of the E. Siberian and Chukchi Seas. This set-up produces extremely high local PP in the AW with maximum annual rates of $\sim 400\text{--}800 \text{ g C m}^{-2} \text{ a}^{-1}$ (Sambrotto et al., 1984; Piatt and Springer, 2003). These rates rival the highest found anywhere in the ocean.

In addition to the Anadyr Water (AW) inflow into the Arctic, Bering Shelf Water (BSW) flows northward in central Bering Strait, and there is also a northward flow of Alaska Coastal Water (ACW) in eastern Bering Strait (Woodgate et al., 2006). BSW has moderate nutrient concentrations (pre-bloom nitrate $\sim 15 \mu\text{M}$), and ACW has low nutrient concentrations (pre-bloom nitrate $<10 \mu\text{M}$; Fig. 3) such that the average pre-bloom nitrate concentration in the Pacific inflow is probably $\sim 20 \mu\text{M}$ (e.g. Codispoti et al., 2009). For example, early spring data from central Bering Strait suggest pre-bloom nitrate concentrations of $\sim 20 \mu\text{M}$ (Cooper et al., 2006; Table S1). Low-salinity, low nitrate ACW (Fig. 3) dominates the flow in eastern Bering Strait during the summer and autumn (Woodgate and Aagaard, 2005; Fig. S6). During these seasons, ACW can be found in the Chukchi Sea adjacent to the coast in a banded flow that follows the topography with higher nutrient AW and BSW, and their modifications occurring in an adjacent offshore band (Fig. S1).

The high productivity region in the western Bering Strait region arising from the almost continuous supply of nutrients in AW behaves more like a chemostat than a spring-bloom system (e.g. Sambrotto et al., 1984). This makes it impossible to accurately estimate NCP solely from local seasonal changes in nutrient concentrations within the AW. In addition, because the inflow of low-nutrient ACW through eastern Bering Strait occurs mainly in summer and autumn, there is a seasonal displacement of higher nutrient water masses by ACW in eastern Bering Strait. This can

cause nutrient concentrations in eastern Bering Strait to decrease during the vegetative season in the absence of NCP. These factors, together with the heterogeneous water mass structure, complicate estimation of NCP from changes in nutrients in the Bering and Chukchi Southern sub-regions (Fig. 1b).

2.5. Riverine impacts on nutrients

The Arctic Ocean receives $\sim 10\%$ of global river runoff and is the “most riverine of the world’s oceans” (Carmack et al., 2006). Nutrient inputs from rivers are, however, small compared to the advective inputs from the Atlantic and Pacific Oceans (e.g. Codispoti and Owens, 1975), and may support only $\sim 10\%$ of total NCP (Gordeev et al., 1996; Gordeev, 2000). The rivers have indirect effects on PP and NCP by inducing estuarine circulations that help to transport and concentrate nutrients in shelf bottom waters as explained by Redfield et al. (1963). Basically, the offshore surface flow induced by runoff is compensated by an onshore flow of higher nutrient sub-surface waters. The nutrient concentrations in the sub-surface onshore flow are then further enriched by sinking and regeneration of organic material from the offshore surface flow (see Fig. S7). Some of the nutrients carried onto shelves in sub-photoc zone layers by estuarine circulation and upwelling during the warm months can subsequently be introduced to the photic zone by wintertime convection. River outflows can also accelerate ice-retreat thereby lengthening the vegetative season (Antonov, 1957). A negative impact of rivers is reduced light penetration due to their transports of suspended particulate matter and colored dissolved organic matter (Hill, 2008). River runoff can also impact nitrate/phosphate ratios. For example, near the mouth of the Mackenzie River phosphate is exhausted well before nitrate depletion (Carmack and Macdonald, 2001; Fig. 2). This is not the case in the adjacent photic zones of the Beaufort Sea and in the Amerasian Basin because of the dominance of waters originating in the Pacific (Fig. 2).

2.6. Iron limitation

With the exception of the Deep Bering Sea (Aguilar-Islas et al., 2007), iron does not appear to be a major limiting factor. Future reductions in ice-cover and its associated iron transport could diminish the iron supply to the photic zone of the Polar Basins (Carmack et al., 2006; Measures, 1999), but there would, of course, still be inputs from the atmosphere, from rivers, and via transport from sediments and sub-surface waters.

2.7. Nutrient losses

Loss of the inputs of nutrients to the photic zone arise, in part, from physical processes (subduction, convection) that can transport relatively high salinity high nutrient waters below the low salinity ambient surface waters. Stripping of nutrients from the photic zone during the ~ 10 year residence time of Arctic surface waters (Östlund, 1982; Macdonald et al., 2004) due to the sinking of biogenic matter is also important. Near-zero nitrate concentrations prevail in the upper ~ 50 m of the Northern Beaufort Sea sub-region even during winter. Since these data (Fig. 5) come from a region close to the boundary of the Amerasian Basin (particularly the Canada sub-basin), we presume that these conditions extend into that region as well. Factors that contribute to the low nitrate concentrations in the Northern Beaufort Sea and Amerasian Basins include downwelling of low nutrient surface waters under the influence of the Beaufort High.

Waters outflowing from the Eurasian Basin in the E. Greenland Current have pre-bloom nitrate concentrations in the surface layer of about $5 \mu\text{M}$ (Packard and Codispoti, 2007), and in the Northeast

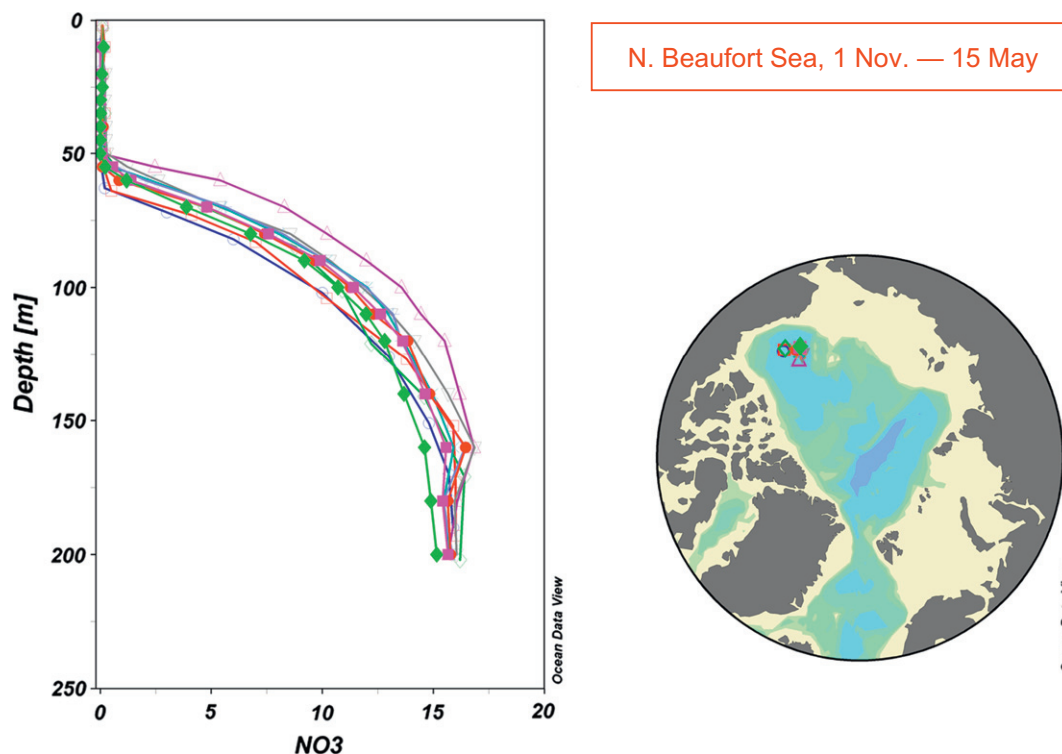


Fig. 5. Vertical nitrate (in μM) profiles in the Northern Beaufort sub-region during winter.

Water Polynya (NE Greenland Shelf) this nitrate is consumed by phytoplankton growth during summer (Kattner and Budéus, 1997). Nutrients in the Canadian Archipelago outflow are enriched by upwelling and tidal mixing in some areas such as the North Water Polynya and Lancaster Sound (Tremblay et al., 2002; Stirling, 1980). In general, pre-bloom photic zone nitrate concentrations in the Archipelago are $\sim 10 \mu\text{M}$, (Figs. S8–S11) and stratification limits uptake to much shallower depths than in the Nordic and Barents seas.

2.8. Types of production

To compare our estimates of NCP with more common estimates of PP, it is necessary to distinguish between different types of primary production. *Gross Primary Production* (GPP) is defined as photosynthesis that does not account for contemporaneous algal respiration or the metabolism of heterotrophic organisms. *Net Primary production* (NPP) is GPP minus algal respiration. *Net community production* (NCP) is defined as GPP minus algal and heterotrophic respiration.

There are voluminous literature discussions on whether PP determined by ^{14}C incubations approximates GPP, NPP or NCP (e.g. Peterson, 1980; Marra, 2009; Williams, 1993a,b). There is some agreement that the results of typical ^{14}C incubations lie somewhere between GPP and NPP, tending towards GPP at lower PP rates and shorter time intervals and towards NPP at higher rates and longer intervals (e.g. Le Bouteiller, 1993). This issue is not settled, and the tendencies may, in part, be a function of species composition (e.g. Williams, 1993b). In addition, some ^{14}C incubations may produce a result between NPP and NCP for the community in the incubation bottle (e.g. Marra, 2009).

Primary production rates obtained via ^{14}C incubations are often referred to simply as primary production and extended in different ways to provide an estimate of total daily primary production for incubation periods shorter than 24 h. Marine scientists generally mean this type of PP when they refer to “primary production”

without further qualification. The companion paper of Hill et al. (2013) restricted its use of ^{14}C incubation data to experiments lasting between 20–24 h, and these authors suggests that these rates may be closest to NPP.

For any given system the following inequality should apply $\text{GPP} \geq \text{NPP} \geq \text{NCP}_{\text{bottle}} \geq \text{NCP}_{\Delta\text{nut}}$. This inequality is an extension of one provided by Williams (1993b) insofar as it makes an explicit distinction between NCP determined in bottle incubations of 24 h or less ($\text{NCP}_{\text{bottle}}$) and NCP values determined from maximum nitrate and phosphate draw-downs in a region’s water column over the vegetative season ($\text{NCP}_{\Delta\text{nut}}$). $\text{NCP}_{\text{bottle}}$ can be integrated to provide an annual rate and $\text{NCP}_{\Delta\text{nut}}$ should approximate an annual rate. We justify this extension for three reasons: (1) An incubation bottle cannot contain larger organisms that contribute to heterotrophic respiration. Indeed, organisms larger than a few hundred microns in diameter are often purposely excluded. The difference in respiration may, however, be small since somewhere between 90% and >99% of total water column respiration generally occurs in size fractions $<100 \mu\text{m}$ (e.g. Robinson and Williams, 2005). (2) Mixing events during the vegetative season (e.g. Sakshaug and Slagstad, 1992) can entrain nutrients that have been taken up earlier in the growing season, sunken beneath the photic zone as organic matter and been re-regenerated. Such nutrients could contribute to $\text{NCP}_{\text{bottle}}$ more than once, but would be registered only once by $\text{NCP}_{\Delta\text{nut}}$. Mixing events can cause dramatic increases in NCP ($\sim 40\%$) in portions of the Barents Sea south of the Polar Front (Sakshaug, 1997; Sakshaug and Slagstad, 1992), but it is not clear what portion of this fraction is due to regeneration of nutrients vs. the “mining” of “new” nutrients from deeper in the water column. (3) Our methodology computes seasonal nutrient draw-down to the deepest level where such draw-downs can be observed including sub-photoc zone depths in favor of attempting to assess vertical nutrient transports into the photic zone. Nutrient regeneration that occurs below the photic zone or mixed layer but within the integration depth during the vegetative season may therefore mute the signal of total uptake.

Although, $NCP_{\Delta_{nut}}$ should, *theoretically*, be about 5–40% less than NCP_{bottle} , methodological issues narrow the gap. For example, most ^{14}C PP incubations neglect that fraction of total carbon fixation that is returned to the incubation vessel as dissolved organic matter (DOC) (Gosselin et al., 1997; Vernet et al., 1998). In general, this release is ~15% of net particulate primary production (e.g. Baines and Pace, 1991; Jackson, 1993; Mague et al., 1980; Sakshaug, 1997; Sintes et al., 2010), and will cause the incubation results to be too low by the same amount. In addition, incubation artifacts tend to introduce a low-bias into the results of ^{14}C incubations (e.g. Quay et al., 2010). We will, therefore, assume that, *in practice*, $NCP_{\Delta_{nut}} \approx NCP_{bottle}$.

Dugdale and Goering (1967) introduced the concepts of “new” and “regenerated” primary production based on incubations that employed ^{15}N labeled nitrate and ammonium. In their scheme, *total primary production = new + regenerated production*. Nitrate supported production = new production and was thought to represent uptake of nutrients present at the beginning of the vegetative season or transported into the photic zone from elsewhere. Ammonium supported production = regenerated production and represented that fraction of primary production supported by local regeneration of nutrients. Additional forms of regenerated nitrogen such as urea were not originally included, but some subsequent studies indicate that urea uptake can be ~10–30% of total nitrogen uptake (e.g. Le Bouteiller, 1993; Legendre and Gosselin, 1989; Tremblay and Gagnon, 2009). The supply of “new” fixed nitrogen via nitrogen fixation is also not captured by the methodology, but nutrient distributions and hydrographic conditions in the Arctic suggest that this process should not be important (e.g. Carpenter and Romans, 1991; Codispoti et al., 2005). There are additional complexities that can be found in the literature cited and in other publications, but there is a rough consensus that *total production estimated from ^{15}N incubations \approx PP estimated from ^{14}C incubations* and that *new production \approx NCP*. The reader who is interested in why these ~equivalences exist is referred to the papers of Williams (1993a,b) and Le Bouteiller (1993).

3. Methods

3.1. Nomenclature

$NCP_{\Delta_{nut}}$ within the context of this paper means NCP in $g\ C\ m^{-2}$ based on seasonal draw-downs of phosphate and BigN (\approx nitrate; see next paragraph). Generally, the use of the term NCP within this contribution refers to $NCP_{\Delta_{nut}}$. We express the results as $g\ C\ m^{-2}$ rather than as $g\ C\ m^{-2}\ a^{-1}$ because nutrients taken up during the vegetative season are regenerated during the cold months such that the average annual values of NCP based on changes in nutrients would be ~0. In contrast, productivity estimates based on incubation techniques or chlorophyll concentrations generally yield zero or positive rates and can be integrated over a year to produce an annual rate. The NCP values reported here are annual values in the sense that they are based on estimates of the maximum annual draw-down of a selected nutrient. We assume that it is legitimate to treat our NCP results as annual rates when comparing them to annual rates based on incubations and algorithms for converting chlorophyll distributions into PP rates.

Some of the expeditions listed in the data sources only reported nitrate + nitrite data. This is not a major issue because of the generally low (<0.5 μM) nitrite concentrations in the Arctic (e.g. Codispoti et al., 2005). To combine data from cruises that only reported nitrate + nitrite values, with cruises that reported nitrate data we defined a parameter called “BigN”. This parameter reports the nitrate data if only nitrate data are available, the nitrate + nitrite data when only nitrate + nitrite data are available, and the lar-

ger of the two when both types of data are available. In general, BigN closely approximates nitrate concentrations. Also note that “ESS” is sometimes used to abbreviate East Siberian Sea.

NCPs were calculated using a variety of time periods and integration depths for data organized into 100×100 km grid cells (see Section 3.5) and by sub-region (see Section 3.6). In general, the largest NCP values arising from the ensemble of depths and time periods were assumed to be the best estimators of total NCP during the vegetative season. The maximum values based on changes in BigN are referred to as “MaxNCP-N”, and the maximum phosphate based values are referred to as “MaxNCP-P”.

3.2. Study region and sub-regions

In this study, the Arctic Marine System (AMS) means that portion of the marine environment north of $65^{\circ}N$ including the Bering Sea as far south as $60^{\circ}N$ but excluding the Baltic Sea (Fig. 1b). The companion papers of Matrai et al. (2012) and Hill et al. (2013) divide the AMS into 13 sub-regions. We provide NCP estimates for all. In addition, we have sub-divided the Arctic Basin sub-region into the Amerasian and Eurasian sub-basins that lie on either side of the Lomonosov Ridge (Fig. 1b). This is because the nutrient regimes in these two sub-basins differ significantly. As already noted, photic zone nutrient concentrations in much of the Eurasian Basin are not depleted during the vegetative season (Figs. 4a–c and S2) whereas the Northern Beaufort Sea and adjacent Amerasian Basin contain nitrate depleted upper layers even in winter (Fig. 5).

The AMS could be further subdivided to accommodate meso-scale features such as the PP regimes near river mouths and polynyas. Also, note that our regional definitions do not necessarily map one to one with definitions employed in other investigations such that detailed comparison of our results with other studies may require some geographic adjustments.

3.3. Nutrient databases and data quality

The nitrate, nitrate + nitrite, and phosphate data employed in this analysis came from the following databases: An Arctic nutrient data base (ARC-NUT) assembled under the direction of G. Cota and L. Pomeroy (<http://data.eol.ucar.edu/codiac/dss/id=62.015>), a EUROCEANS database (<http://www.eur-oceans.eu/integration/wp2.2>), an initial version (2009) of the CARINA database http://cdiac.ornl.gov/oceans/CARINA/Carina_inv.html, and the Hydrochemical Atlas of the Arctic Ocean (Colony and Timokhov, 2001). These data were supplemented with observations from the Western Arctic Shelf-Basins Interaction Program (Codispoti et al., 2005, 2009), data from the Fram III expedition (Packard and Codispoti, 2007), data from the Canadian Archipelago supplied by F. McLaughlin, and data from a recent expedition to the Canadian Archipelago and Baffin Bay supplied by K. Falkner.

Significant portions of the archived nitrate, nitrate + nitrite and phosphate data were dubious and were excluded from the final data base. Whenever possible nutrient values from depths >300 m were examined to see if they were in accord with high-quality historical data from the same region. In cases where the historical data suggest little temporal variability (e.g. deep water in the Canada Basin), stations that had deep values more than ~10% different from the expected values were rejected. The ARC-NUT database did not include deep values, and many stations in all databases were too shallow to apply this test. Other criteria included rejection of data that produced jagged vertical profiles, values well outside of the expected range for a given region based on data from cruises that were known to have produced high-quality data, and implausible nitrate to phosphate ratios.

A large ensemble of data from the eastern Arctic contained extremely low nitrate and phosphate values suggesting an error

during unit conversions or data encoding and these values were excluded. An ensemble of data with implausibly high nitrite values that cast into doubt the accompanying nitrate data was also rejected. After initial editing, individual cases that yielded implausible NCPs were investigated to see if the dubious results might be related to questionable data. For example, an unusually high NCP from one 100×100 km grid cell in the Nordic Seas, revealed a station that had winter phosphate values 25% higher than the mean winter concentrations for the Nordic Seas and that were not in concert with nearby data from other expeditions, so these data were rejected.

Completely quantitative protocols for accepting or rejecting data were not possible, and we had to also draw on long experience in working with Arctic nutrient data. Interested investigators can, however, compare the accepted phosphate and BigN data used to compute NCP with the data in the original sources since the accepted data are available from the senior author (LAC) and have been submitted to the National Oceanographic Data Center (<http://www.nodc.noaa.gov/archive/arc0034/0072133/1.1/data/0-data>). Figs. 2, 6a and b display the phosphate and nitrate data that survived the editing process. The nitrate + nitrite data are shown in Figs. S12 and S13.

3.4. Converting nutrient draw-downs to $NCP_{\Delta_{nut}}$ and to total primary production

Atomic Redfield regeneration ratios of 106:16 (6.62) for $\Delta C / \Delta \text{BigN}$ –nitrogen and 106:1 for $\Delta C / \Delta \text{phosphate}$ –phosphorus (Anderson, 1995; Redfield et al., 1963) permit conversion of BigN and phosphate draw-downs per square meter into $NCP_{\Delta_{nut}}$ as g C m^{-2} . Anderson and Sarmiento (1994) suggest slightly higher

ratios of ~ 7.31 and ~ 117 for C:N and C:P, respectively. Use of the latter ratios would increase NCP values by $\sim 10\%$ when expressed as carbon. The subsurface regeneration ratio for N/P is remarkably constant at $\sim 16:1$ (e.g. Anderson, 1995; Anderson and Sarmiento, 1994). Over short time intervals, Redfield C/N/P uptake ratios can vary significantly, but the selected values may be approximately correct when averaged over the vegetative season (Hoppema and Goeyens, 1999). Since several studies (e.g. Anderson, 1995; Anderson and Sarmiento, 1994; Redfield et al., 1963) suggest that bulk sub-surface regeneration ratios are reasonably constant, and since these ratios are the products of regeneration of the NCP that supports a flux to depth, it is reasonable to suggest that Redfield ratios can be employed to convert phosphate and BigN draw-downs into carbon units.

Several authors suggest phytoplankton C:N uptake ratios significantly higher than 6.62 (e.g. Sambrotto et al., 1993) when comparing nitrate draw-downs with dissolved inorganic carbon draw downs (DIC). This excess carbon uptake can be rationalized with the ocean's subsurface "Redfieldian" stoichiometry if it is largely related to surface layer accumulations of labile carbon-rich material (including DOC) that are largely re-mineralized in surface waters (Kähler and Koeve, 2001). Koeve's (2004) re-analysis casts doubt on the overall significance of excess C uptake during the spring bloom in the North Atlantic when NCP is high. He suggests that high net C:N uptake ratios tend to occur during post-bloom conditions when the export of the organic material to depth should be low and when the ratio of new to total productivity as determined by ^{15}N incubations is low.

Interpretation of our $NCP_{\Delta_{nut}}$ values is relatively straightforward. They represent our best estimate of the maximal draw-down of BigN and phosphate during the vegetative season converted to

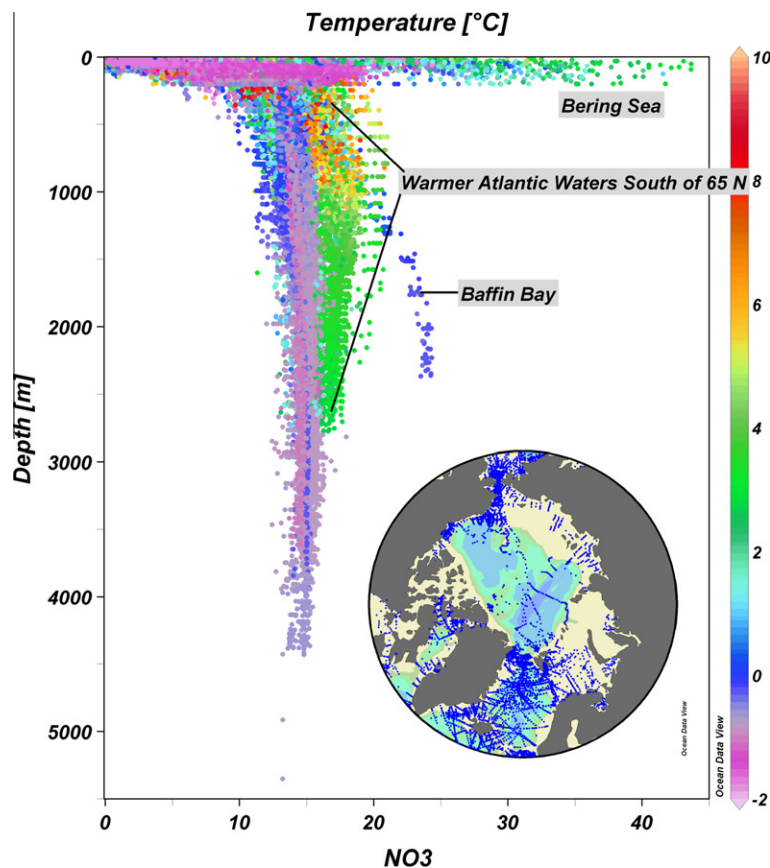


Fig. 6a. Nitrate concentrations (μM) vs. depth, color coded by temperature ($^{\circ}\text{C}$) from the data base employed in this analysis. The higher concentrations in warmer subsurface waters, are found to the south of the topographic features that separate the Nordic Seas from the North Atlantic.

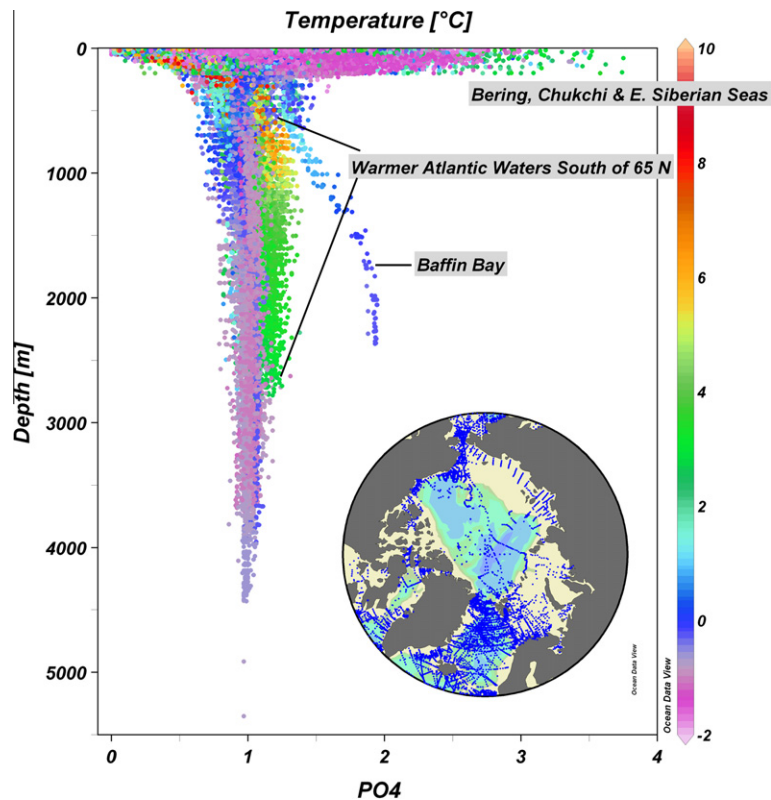


Fig. 6b. Phosphate concentrations (μM) vs. depth, color coded by temperature ($^{\circ}\text{C}$) from the data base employed in this analysis. The higher concentrations in warmer subsurface waters, are found to the south of the topographic features that separate the Nordic Seas from the North Atlantic.

carbon units by the employment of Redfield ratios. In theory, these values should be smaller than $\text{NCP}_{\text{bottle}}$ or new production estimated from incubations, but methodological problems with incubations blur this distinction (see Section 2.8). Since $\text{NCP}_{\Delta_{\text{nut}}}$ should be similar to new production, it should be useful for setting a limit on the amount of organic matter that can be exported from the surface layers to depth (e.g. Eppley and Peterson, 1979).

To convert our $\text{NCP}_{\Delta_{\text{nut}}}$ estimates to PP as estimated by ^{14}C incubations we employed the f -ratio concept. Eppley and Peterson (1979) defined this ratio as new production/total primary production. If one accepts that total production is $\approx\text{PP}$ (see Section 2.8.), then the f -ratio can also be defined as (new production $\times 6.62$)/PP (PP as determined by ^{14}C incubations) where 6.62 is the atomic C:N Redfield ratio during uptake (Le Bouteiller, 1993). Since new production is similar to NCP (see Section 2.8.), we can say that the f ratio is $\approx\text{NCP}/\text{PP}$ (estimated by ^{14}C incubations) and that $\text{NCP}/f\text{-ratio} \approx \text{PP}$ as determined by ^{14}C incubations.

3.5. NCP calculations by 100×100 km grid cell

To facilitate comparison of NCP values based on nutrient draw-downs with other estimates and to combine data from different sources in a geographically consistent way, data were organized by 100×100 km grid cells using the National Snow and Ice Data Center's Equal-Area Scalable Earth Grid (EASE-Grid). The available data were interpolated (linearly) and extrapolated to fill all 1 m depth bins within the selected integration depth. Extrapolations were permitted only when the data were likely to be in a homogeneous layer. For example, if the shallowest observation was at 5 m, it was assumed that the value at the sea surface was the same as the value at 5 m. Integrated nutrient values for a grid cell were calculated by summing trapezoidal sections of the profile that were shaped by available data such that a trapezoid spanned at least

one meter. Summer and pre-bloom values for BigN and phosphate were independently integrated over depth whenever sufficient observations were available.

The depths to which net nutrient uptake can be observed vary significantly within the AMS. To account for these differences, NCPs were calculated by integrating nitrate and phosphate differences to depths of 25, 30, 50, 60, 100 and 150 m whenever sufficient data were present. Data sufficiency criteria varied by integration depth (Table 2). Because of regional differences in the onset and end of net phytoplankton growth, we calculated integrated BigN and phosphate values over the six depth ranges, for three "winter periods" and two "summer periods" (Table 3) that were used as proxies for the examination of pre-bloom (winter) and post-bloom (summer) conditions. The "long summer" period (5 July–29 September, year days 186–272) matches the summer period employed in the companion papers by (Matrai et al., 2012; Hill et al., 2013). Subtracting integrated summer values from integrated winter values produced BigN and phosphate draw-downs during the vegetative season. These draw-downs were then converted into NCP in g C m^{-2} over the vegetative season by employing Redfield ratios.

Rather than decide the appropriate integration depth or the appropriate periods for winter and summer *a priori*, the integration depth and time interval that yielded the highest NCPs values (MaxNCP-N and MaxNCP-P) based on changes in BigN and phosphate were assumed to be most appropriate. However, integrations that could not be performed to depths of at least 50 m were rejected for the Nordic and Barents seas because of the clear evidence that seasonal nutrient uptake signals extend significantly deeper in these regions (Figs. S3 and S4). In addition, integrations to 100 and 150 m were only accepted for the Nordic and Barents seas. In the other regions phytoplankton nutrient uptake below ~ 60 m is small or absent and integrations to 100 and 150 m could be aliased by

Table 2

Data quantity and distribution criteria for accepting integrations for the 100×100 km grid squares.

| Integration depth | Minimum number of observations | Deepest value allowed | Maximum separation ^a |
|-------------------|--------------------------------|-----------------------|---------------------------------|
| 25 | 3 | 30 | 10 |
| 30 | 3 | 35 | 10 |
| 50 | 4 | 60 | 15 |
| 60 | 4 | 70 | 15 |
| 100 | 5 | 125 | 30 |
| 150 | 5 | 175 | 40 |

^a Maximum distance permitted between values that define the bottom boundary of the integration depth.

Table 3

Dates for the winter and summer periods employed in calculations of net community production.

| Winter periods | Year day interval | Calendar dates |
|-----------------------|-------------------|------------------------|
| Short Winter | 335–059 | December 1–28 February |
| Medium Winter | 319–091 | November 15–1 April |
| Long Winter | 305–135 | November 1–15 May |
| <i>Summer periods</i> | | |
| Short Summer | 232–272 | August 20–September 29 |
| Long Summer | 186–272 | July 5–September 29 |

small systematic errors or by temporal variability in water masses. Finally “long winter” (1 November–15 May; Table 3) was not permitted for the Barents, Bering, and Nordic Seas because this winter period could overlap the relatively long vegetative seasons in these regions.

Pre-bloom data were sparse. A practical reason for providing a choice of “winter” and “summer” intervals is that much of the pre-bloom data from the Polar Basins comes from astronomical spring when there is sufficient light to facilitate aircraft operations, but before the onset of significant PP. Listings of the maxNCP-P and maxNCP-N values for the grid cells that produced results plus the identifications and locations of the cells are included in the supplementary materials (Tables S2 and S3).

3.6. NCP by sub-region

To calculate NCP on a grid cell basis requires a union of winter and summer data within a grid. This requirement reduces coverage. For this reason, we also examined phosphate and BigN data pooled over entire sub-regions (Fig. 1b) for the time periods listed in Table 3. If sufficient data are available from a given sub-region in relation to its water mass variations, temporal and spatial differences in water masses might be averaged out yielding a reasonable estimate of NCP.

To obtain regionally averaged phosphate and BigN draw-downs from data for an entire sub-region the data were first binned and averaged into 5 m depth intervals. Then, the binned data from all grid cells that contained data from the selected region and time periods (Table 3) were arithmetically and geometrically averaged to produce profiles for conditions at the beginning (~winter) and end (~summer) of the vegetative season. Subtracting the summer values from the winter values for each bin, integrating the differences over depth until the difference was maximal, and taking the time period combination yielding the largest result gave estimates of maxNCP-P and maxNCP-N. The same combinations of winter and summer periods employed to determine maxNCP-N and maxNCP-P for the 100×100 km grid squares were examined (Table 3) to estimate maxNCP-N and maxNCP-P via this procedure. All possible combinations of winter and summer periods were

examined, and the combination that produced the highest maxNCP value was assumed to be the best estimator of maxNCP. In general, the winter and summer combination that produced the highest NCP value involved the shortest or next to shortest available period for winter and the shortest available period for summer as one might expect. In some cases the longer of the two definitions of summer provided higher NCP values. We assumed that this was because the larger amount of data associated with these cases helped to average out errors, and regional and temporal variations and chose the larger NCP values. In some cases initial integration depths for maxNCP were reduced because an ensemble of stations produced an integration depth that was too deep for a sub-region's average topography or because sparse data from deeper in the water column caused unrealistic results. We calculated NCP using both arithmetic and geometric means for the data in each 5 m depth bin. Within our data, it is possible that geometric means suppress high post-bloom values more than high pre-bloom values. This would tend to make the NCP values based on geometric means too high, but the differences between the NCP values estimated from arithmetic and geometric means were generally small (e.g. Figs. 7–13). Further discussions of how these data were employed to estimate NCP is given on a sub-region by sub-region basis in Section 4.

3.7. Qualitative NCP estimates

We also made qualitative estimates of NCP for each sub-region, based on inspection of the available data and on values in the literature. This was done to guard against unrepresentative quantitative results that could arise from sparse data or from features that our methodology could not properly take into account. In the Bering and Chukchi Southern sub-regions the qualitative estimate is likely to be superior to our quantitative estimates because of the complications noted in Section 2.4. In some other sub-regions, lack of data also necessitated a qualitative estimate. We will point out such cases as we discuss our estimates for each sub-region. The profiles and sections examined to arrive at the qualitative NCP estimates include Figs. 3–5 and most of the Supplementary figures.

3.8. Sections

We present several “sections” in the Supplementary figures. Sometimes we have aggregated data from several expeditions conducted in different years in these sections. Such sections are obviously not synoptic. They are merely a convenient way to present the data that should give some idea of mean conditions.

3.9. Statistics

Applying common statistical estimators to our results is problematic. In part, this is because our data editing process depended to an extent on subjective judgements. In addition, there are almost certainly systematic differences in NCP within our sub-regions, and this may also be the case for data from 100×100 km squares that lie near boundaries. The standard deviations given in Table 4 are calculated as sample standard deviations (s) with the number (n) of observations taken to be the number of grid square results available for each calculated value. These deviations give some idea of the dispersion about the mean value, but should be interpreted with caution. The same caveats apply when we discuss the standard error of the means ($SEM = s/\sqrt{n}$). Fig. S14 shows a regression of MaxNCP-P vs. MaxNCP-N. This is a Type II linear regression calculated by employing a program made available by E. Peltzer (<http://w3eos.who.edu/12.747/resources/lsq/lsqfitma.m>).

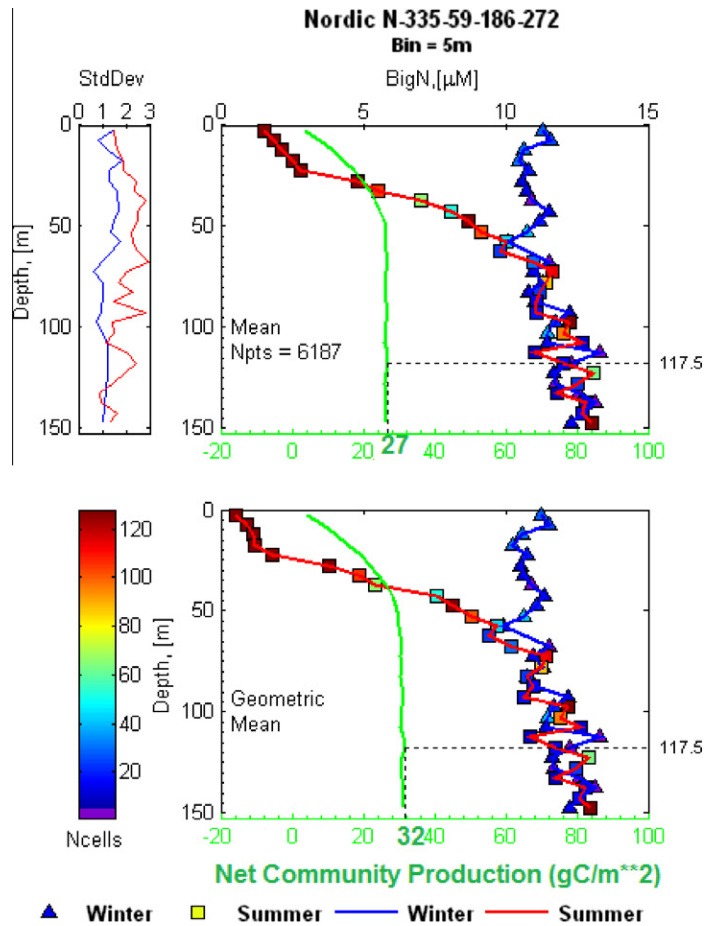


Fig. 7. Average winter (1 December–28 February) and summer (5 July–29 September) BigN values (in μM) in the Nordic Seas sub-region based on data binned by 5 m depth intervals. $\text{MaxNCP-N} = 27 \text{ g C m}^{-2}$ based on the maximum integrated difference between the winter and summer arithmetic means for BigN.

4. Results

4.1. General

In this section, we will “tour” the AMS and make estimates of NCP ($\text{NCP}_{\Delta\text{nut}}$). Whenever possible, we shall compare the NCP results from the three complementary approaches described in Section 3. Briefly, these three approaches are as follows: (1) the qualitative interpretation of nutrient distributions (supplemented by the literature); (2) NCP results from maxNCP-P and maxNCP-P values based on aggregating the data by sub-region, and (3) NCP obtained by averaging the maxNCP-N and maxNCP-P data available in $100 \times 100 \text{ km}$ squares from each sub-region (Table 4). As noted earlier, some of the figures and data that informed the qualitative estimates are included in the [Supplementary material](#). In several cases, the results for a given sub-region had to be restricted to the qualitative approach because of sparse data. For the reasons given in Section 2 and discussed further below, the qualitative approach may be superior for the Bering Sea and Chukchi southern sub-regions.

4.2. Nordic and Barents seas

In the Nordic and Barents seas, pre-bloom BigN and phosphate concentrations (particularly in the Nordic Seas) are relatively uniform over several hundred km length scales and over depth scales in excess of 100 m. Inspection of the pre and post bloom data in [Figs. S3 and S4](#) and integrating the seasonal differences over depth

suggests NCP values for the Nordic and Barents seas of $\sim 25\text{--}45 \text{ g C m}^{-2}$.

The NCP calculations based on aggregating data over the entire Nordic Seas sub-region suggest maxNCP-N and maxNPP-P values ([Figs. 7 and S15](#)) of $\sim 27 \text{ g C m}^{-2}$. The mean values of max-NCP-N and max NCP-P values based on the data calculated from the $100 \times 100 \text{ km}$ squares were both 31 g C m^{-2} (Table 4). If normal statistics are applied (see Section 3.9), the standard error of this mean (SEM) values would be $\sim 2 \text{ g C m}^{-2}$. Given this calculation and the reasonable agreement between the various estimates (qualitative, data aggregated by sub-region, and averages for the $100 \times 100 \text{ km}$ squares), we suggest an NCP value for the Nordic Seas sub-region of $\sim 30 \pm 5 \text{ g C m}^{-2}$. When the data are aggregated over the entire Barents Sea sub-region, maxNCP-N and maxNCP-P means are 46 and 34 g C m^{-2} respectively ([Figs. 8 and S16](#)). Averaging the data from the available $100 \times 100 \text{ km}$ squares gave a maxNCP-N value of 47 g C m^{-2} with an SEM of 4 g C m^{-2} . The maxNCP-P benefits from more abundant data (25 vs. 14 squares) and is 39 g C m^{-2} with an SEM of 4.4 g C m^{-2} . Based on these calculations we suggest an NCP value for the Barents Sea sub-region of $\sim 40 \pm 10 \text{ g C m}^{-2}$.

4.3. Eurasian Basin and Northern East Siberian Sea + Laptev Sub-regions

Low salinity (<32) and relatively high phosphate ([Fig. S17](#)) waters carrying a Pacific signature commingle with waters of Atlantic origin in the upper layers of the Eurasian Basin, but waters

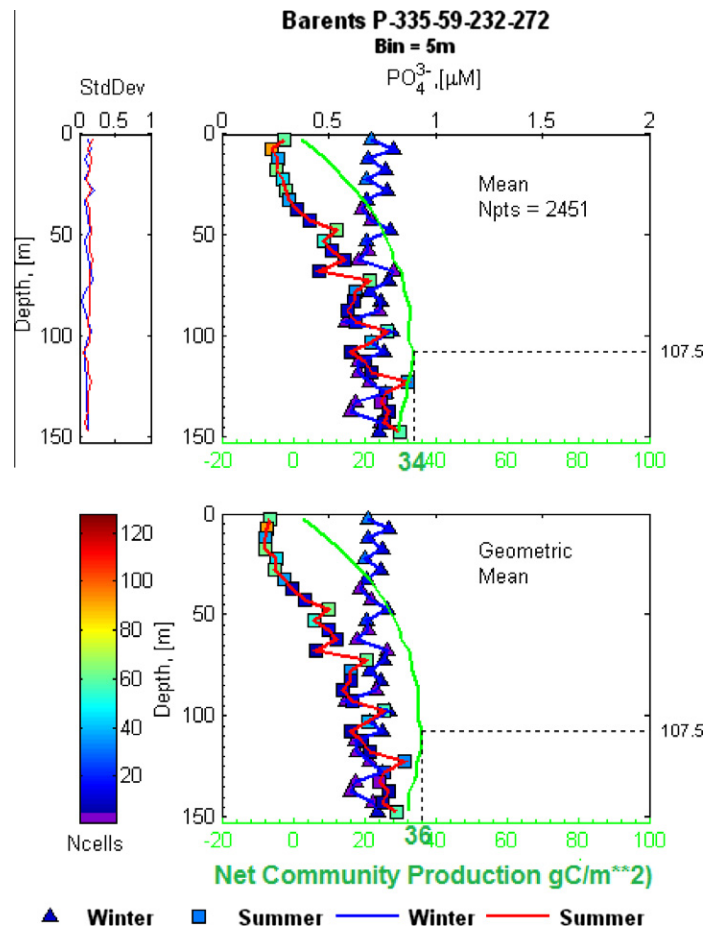


Fig. 8. Average winter (1 December–28 February) and summer (5 July–29 September) phosphate (P) values (in μM) in the Barents Sea sub-region based on data binned by 5 m depth intervals. $\text{MaxNCP-P} = 34 \text{ g C m}^{-2}$ based on the maximum integrated difference between the winter and summer arithmetic means for phosphate.

of Atlantic origin dominate. Regions with higher salinity indicate a higher Atlantic influence and can have nitrate concentration in the upper 20 m in excess of $5 \mu\text{M}$ even in summer (Fig. S2). Because of large water mass related changes in phosphate that extend into the upper 50 m, we relied only on changes in BigN (\sim nitrate) to estimate NCP in the Eurasian Basin. Our qualitative analysis suggested an NCP for the Eurasian Basin of $\sim 10 \text{ g C m}^{-2}$. Data from this region were sparse, but an integration of the difference between summer and winter values aggregated over the sub-region yields a maxNCP-N of $\sim 14 \text{ g C m}^{-2}$ (Fig. 9). The maxNCP-N value based on averaging data from the six available grid squares (Table 4) was 13 g C m^{-2} with an SEM of 3 g C m^{-2} . Packard and Codispoti (2007) and Zheng et al. (1997) present results suggesting that export production near the Atlantic entrances to the Eurasian Basin is $\sim 30 \text{ g C m}^{-2}$, but these results were back-calculated from water column respiration and regeneration rates. Since the Eurasian Basin imports organic matter in the waters that inflow from the Nordic and Barents seas, a rate of 30 g C m^{-2} is likely to be an overestimate of local NCP in the Eurasian Basin. In addition, productivity in the Eurasian Basin may be higher near the Atlantic entrances because of higher nitrate concentrations. We suggest an NCP value for the Eurasian Basin sub-region of $\sim 15 \text{ g C m}^{-2}$.

Data from the Northern ESS + Laptev region are extremely sparse. A lack of pre-bloom data forced us to rely solely on a qualitative estimate. To make this estimate we assumed pre-bloom concentrations of $\sim 5 \mu\text{M}$ for BigN based on the data from $\sim 50 \text{ m}$ in the summer profiles (Fig. S18). The phosphate data were not useful perhaps because of variations in water masses with differing BigN/phosphate ratios. The vertical gradient in the summer BigN

profile suggests that an average of $\sim 2 \mu\text{M}$ of BigN from depths above 50 m is removed by biological uptake during the vegetative season. These values yield an NCP-N of 8 g C m^{-2} . This value is intermediate between the values for the abutting sub-regions (Fig. 1b and Table 5), and would therefore seem reasonable. Nevertheless, the absence of winter data makes the result tenuous. We can only speculate that the NCP value for the ESS + Laptev Northern sub-region is $\sim 8 \text{ g C m}^{-2}$ with a range of $\sim 3\text{--}15 \text{ g C m}^{-2}$.

4.4. Amerasian Basin, Northern Beaufort, and Northern Chukchi Sub-regions

The data from the Amerasian Basin and Northern Beaufort sub-regions are in accord with the hydrographic description given earlier (Section 2): throughout much of this region downwelling under the influence of the Beaufort High, strong stratification, and the residence time of the surface waters combine to deplete surface layer nitrate concentrations even in winter (Figs. 4a–c and 5). Thus, our qualitative analysis suggests that NCP in these two sub-regions should be low ($< 5 \text{ g C m}^{-2}$).

The sparse aggregated data from the Northern Beaufort and Amerasian Basin sub-regions (Figs. 10 and S19) indicate that BigN (\sim nitrate) concentrations in the surface layers are low during winter and summer and gave a maxNCP-N value of $\sim 1 \text{ g C m}^{-2}$ for the Beaufort Northern sub-region, and of $\sim 1 \text{ g C m}^{-2}$ for the Amerasian Basin sub-region. The available Amerasian Basin data suggest significant uptake below 60 m, but we attribute this to differences in water mass composition in our sparse data unrelated to local uptake of nutrients. Similarly, NCPs based on changes in phosphate

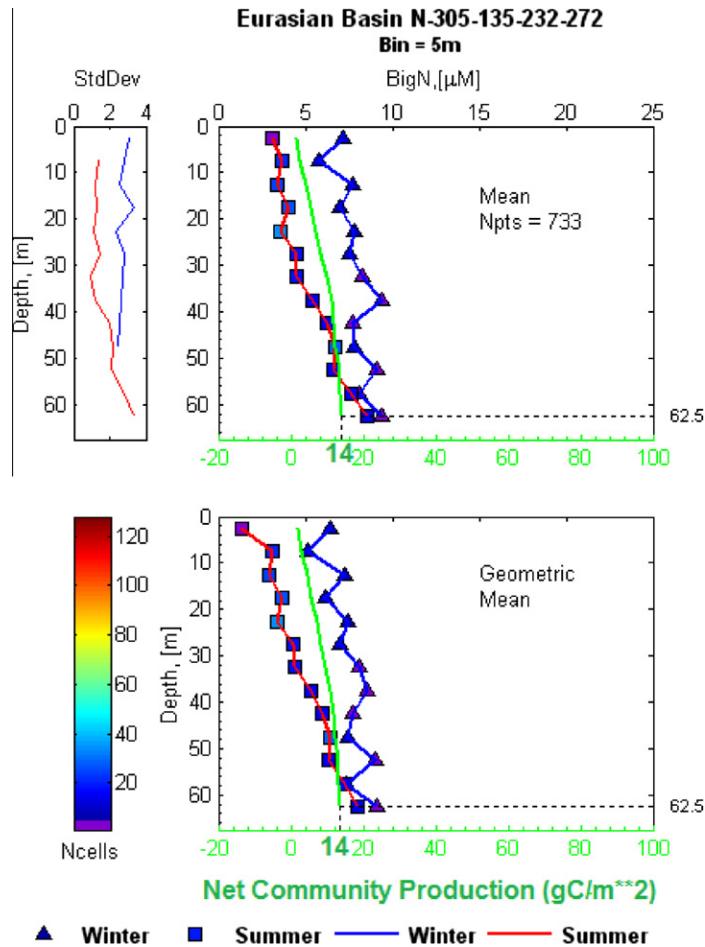


Fig. 9. Average winter (1 November–15 May) and summer (20 August–29 September) BigN values (in μM) in the Eurasian Basin based on data binned by 5 m depth intervals. MaxNCP-N = 14 g C m^{-2} based on the maximum integrated difference between the winter and summer arithmetic means for BigN.

are higher than 2 g C m^{-2} , but phosphate limitation is not likely in this region (Fig. 2). In addition, there are significant water mass related differences in phosphate that complicate interpretation. Only one $100 \times 100 \text{ km}$ grid square from these two sub-regions produced a result. It was a value for maxNCP-N of 4 g C m^{-2} for the Amerasian Basin (Table 4). Bates et al. (2005) suggest an NCP for the Beaufort Northern sub-region based on seasonal changes in dissolved inorganic carbon (DIC) of $2.5\text{--}6.5 \text{ g C m}^{-2}$, but they extrapolated their results to a 120 day growing season which extends the growing period well beyond (~ 2 months) the period when nitrate was depleted. This may be appropriate for DIC based calculations since “excess” carbon uptake can continue after nitrate exhaustion (see Section 3.4), but is not appropriate for direct comparison with our results. Correcting for the growing period lowers the values by a factor of 2–3 yielding a corrected NCP range of $\sim 1\text{--}3 \text{ g C m}^{-2}$. In addition, their results came from the southern boundary of the Beaufort Northern region, which abuts more productive sites. Overall, our estimate for NCP in the Beaufort Northern sub-region is $\sim 1 \text{ g C m}^{-2}$. For the Amerasian Basin, the estimate is $\sim 3 \text{ g C m}^{-2}$. We speculate that these values are not likely to exceed 5 g C m^{-2} and will assign ranges of $0.5\text{--}5 \text{ g C m}^{-2}$ for NCP in both regions.

Data are sparse in the northern Chukchi Sea, and integrations are aliased by differences in water masses. If integrations based on the data aggregated by sub-region for the Chukchi Northern sub-regions are confined to the upper $\sim 20\text{--}40 \text{ m}$, NCP values based on differences between winter and summer BigN and phosphate concentrations are $\sim 5 \text{ g C m}^{-2}$ (Figs. S20 and S21). Because the val-

ues from deeper than $20\text{--}40 \text{ m}$ are higher in summer than in winter, we suspect that these results are low due to water mass differences that are not averaged out in the sparse data. Therefore, an NCP of 5 g C m^{-2} is likely to be a minimum estimate. Two values from $100 \times 100 \text{ km}$ squares yield an average maxNCP-P value of 14 g C m^{-2} for this sub-region. Bates et al. (2005) and Mathis et al. (2009) calculated significantly higher NCP rates within the southern portion of the Chukchi Northern sub-region, based on seasonal changes in the inorganic carbon system. As noted above, they assumed a 120 day bloom period and extrapolated changes in DIC observed during shorter periods. Since nitrate was often exhausted during their summer observations (e.g. Codispoti et al., 2005), we re-calculated their results. Using their observed spring to summer differences in DIC, we obtained an average NCP value of 15 g C m^{-2} (17 values, std. dev. = 17 g C m^{-2}) for the southeastern portion of the Chukchi Northern sub-region that abuts the more productive Chukchi Southern sub-region. Based on these considerations we suggest that the best estimate for NCP in the Chukchi Northern sub-region is $\sim 10 \text{ g C m}^{-2}$ with an estimated range of $5\text{--}20 \text{ g C m}^{-2}$. While an NCP of 10 g C m^{-2} may seem low for any portion of the Chukchi Sea, recall that the Chukchi Northern sub-region as defined herein includes the Chukchi Borderlands and part of the adjacent Amerasian Basin (Fig. 1b).

4.5. Arctic Deep Basin

Because Hill et al. (2013) lumped the Eurasian and Amerasian sub-basins into one Arctic Basin sub-region, we combined our esti-

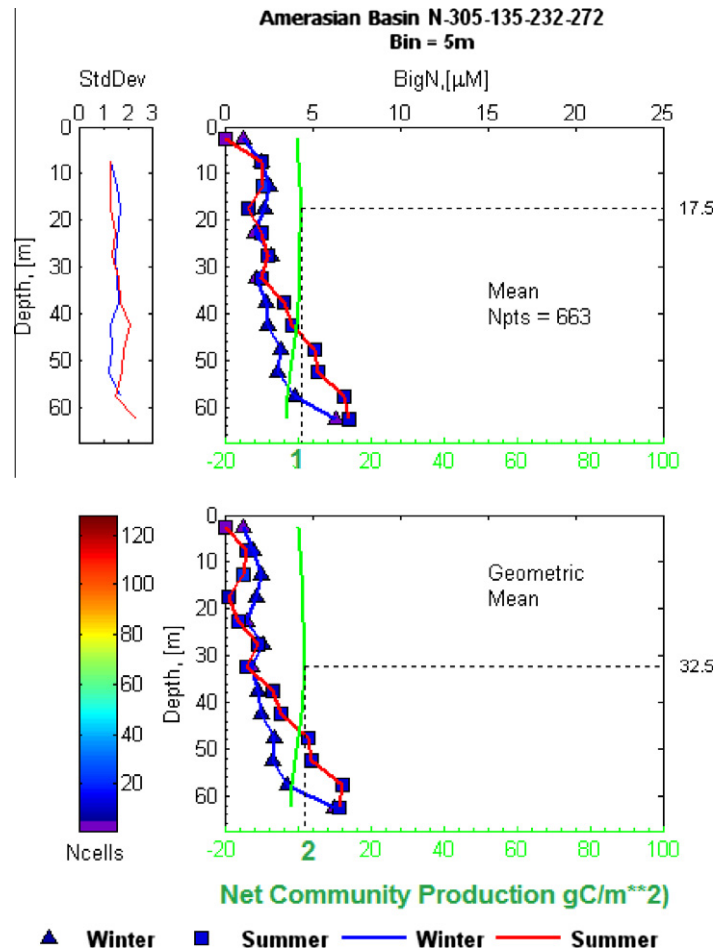


Fig. 10. Average winter (1 November–15 May) and summer (20 August–29 September) BigN values (in μM) in the Amerasian Basin based on data binned by 5 m depth intervals. MaxNCP-N = 1 g C m^{-2} based on the maximum integrated difference between the winter and summer arithmetic means for BigN.

mates for these sub-basins to facilitate comparison. The ratio of the area of the Amerasian Basin sub-region to the sum of the areas of the Eurasian Basin and Amerasian Basin sub-regions shown in Fig. 1b is 0.6. With an NCP value of $\sim 3 \text{ g C m}^{-2}$ for the Amerasian Basin and a value of $\sim 15 \text{ g C m}^{-2}$ for the Eurasian Basin, the area weighted average NCP for the two basins is $\sim 8 \text{ g C m}^{-2}$. A value of 8 g C m^{-2} is low, but significantly larger than Sakshaug's (2004) estimate for the central deep Arctic of $< 1 \text{ g C m}^{-2} \text{ a}^{-1}$. Note, however, that he estimated a range of $5\text{--}30 \text{ g C m}^{-2}$ for total productivity (\approx PP) in the Nansen Basin (part of the Eurasian Basin) but lacked new production data for this region.

4.6. Greenland Shelf

As defined here (Fig. 1b), the Greenland Shelf sub-region includes those portions of the east and west Greenland shelves north of 65°N . In these areas stratification is strong, and nitrate concentrations are relatively low (Figs. S22–S25). Nitrate depleted fresh water inputs are accumulated over this shelf by the dynamics associated with the southward flowing East Greenland Current and the northward flowing West Greenland Current. Over the East Greenland Shelf, low salinity waters exiting the Arctic have low nitrate concentrations even in winter ($\sim 4 \mu\text{M}$) in the upper 50 m (Fig. 11). As the waters travel south in the East Greenland Current, ice-melt and fresh water additions from melting glaciers will enhance these conditions whereas mixing with ambient Atlantic waters will relax them. Over the West Greenland Shelf north of 65°N , winter nitrate concentrations are also low and stratification

is strong, perhaps as a consequence of ice-melt and fresh water from glaciers (Figs. S22–S25). Overall, winter nitrate concentrations in the upper 50 m appear to be $< 5 \mu\text{M}$, and summer draw-downs in the upper 50 m appear to be about $2.5 \mu\text{M}$. These values yield a qualitative annual NCP estimate of $\sim 10 \text{ g C m}^{-2}$. To the south of 65°N , NCP over the Greenland Shelf is likely to approach values found in the Nordic Seas because of the greater influence of ambient Atlantic waters, but this region is outside of the purview of this study.

Integration of seasonal changes in phosphate in data aggregated over the entire sub-region yielded NCP values ranging from 2 to 17 g C m^{-2} . Given that this region can contain a mixture of Pacific and Atlantic influenced waters, we did not rely on the phosphate based integrations for the aggregated data. Integrated changes in BigN concentrations in the aggregated data suggest a maxNCP-N of $\sim 8 \text{ g C m}^{-2}$ (Fig. 11) if the integrations were restricted to the upper 52 m using the definition of “summer” that begins on 5 July (Table 3; year days 186–272). Since including data taken as early as 5 July may include cases where nutrients have not yet reached minimum values, this value is probably low. There was some apparent uptake below 52 m, but this was interpreted as a change in water mass composition not directly related to regional NCP. MaxNCP-N data from grid squares (Table 4) suggest a mean value of 12 g C m^{-2} with an SEM of $\sim 3 \text{ g C m}^{-2}$ and a maxNCP-P value of 15 g C m^{-2} with an SEM of $\sim 3 \text{ g C m}^{-2}$. These averages exclude anomalously large values (max NCP-P = 40 g C m^{-2} , max NCP-N = 56 g C m^{-2}) from one grid square within this sub-region, but at the boundary of this sub-region with the Nordic Seas sub-region.

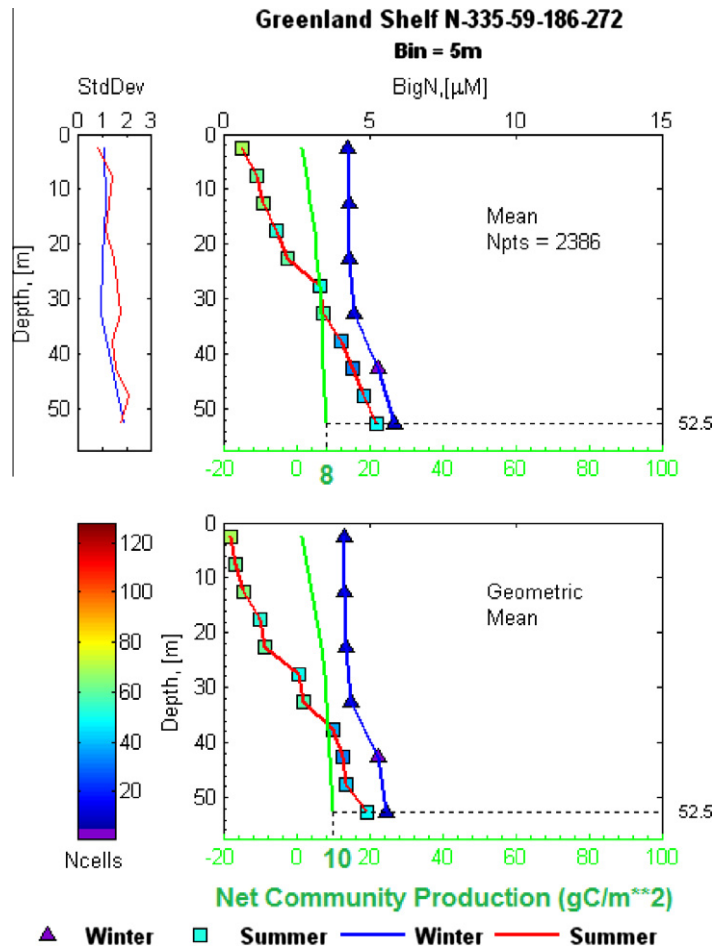


Fig. 11. Average winter (1 December–28 February) and summer (5 July–29 September) BigN values (in μM) for the Greenland Shelf based on data binned by 5 m depth intervals. MaxNCP-N = 8 g C m^{-2} based on the maximum integrated difference between the winter and summer arithmetic means for BigN.

Inclusion of this grid square would have raised this sub-region's average maxNCP-P from 15 to 16 g C m^{-2} , and its average for maxNCP-N from 12 to 16 g C m^{-2} . These results suggest that the average NCP for the Greenland Shelf sub-region could plausibly range from ~ 5 to 25 g C m^{-2} and that a reasonable estimate would be $\sim 15 \text{ g C m}^{-2}$.

4.7. Canadian Archipelago

As defined here (Fig. 1b), the Canadian Archipelago sub-region is widespread and includes most of Baffin Bay. Within this sub-region there is a significant variation in pre-bloom nitrate concentrations. Overall, vertical profiles and sections (Figs. S8–S11 and S26–S27) suggest that pre-bloom nitrate concentrations in the upper $\sim 50 \text{ m}$ of the water column are $\sim 10 \mu\text{M}$ and that most of the seasonal nitrate uptake is restricted to the upper 50 m . Inspection of these figures suggested that approximately $8 \mu\text{M}$ of nitrate was removed from the upper 25 m , $4 \mu\text{M}$ from 25 – 50 m , and perhaps $1 \mu\text{M}$ from depths of 50 – 150 m . Such removal yields an NCP of 32 g C m^{-2} .

When the data were aggregated over the entire sub-region, integration over depth of the seasonal differences in BigN and phosphate suggested a maxNCP-P of 22 g C m^{-2} and a maxNCP-N of 27 g C m^{-2} (Figs. 12 and S27). The average maxNCP-N based on data from 9 grid squares was 32 g C m^{-2} with an SEM of $\sim 2 \text{ g C m}^{-2}$ (Table 4). The average for maxNCP-P from 10 grid squares was 44 g C m^{-2} with an SEM of $\sim 5 \text{ g C m}^{-2}$ (Table 4). The average of the four quantitative results is 31 g C m^{-2} , similar to

the result of the qualitative analysis. Nutrient supplies via upwelling and tidal mixing (Stirling, 1980) may be important in this sub-region, and these processes could be insufficiently resolved by our data, so we suggest that NCP in the Canadian Archipelago sub-region is $\sim 35 \pm 15 \text{ g C m}^{-2}$. Sakshaug's (2004) estimate for the Canadian Arctic (Table 1) is much smaller, but he included productive polynya's in a separate category and his definition of the Canadian Arctic was considerably different than ours (Fig. 1b).

4.8. Southern Beaufort

The range of the few pre-bloom nutrient concentrations available from the Beaufort Southern sub-region is high (Fig. S28). This variability could reflect the variability in nutrient concentrations in the "upstream" water masses in the adjacent Chukchi Sea, the influence of the Mackenzie River (Fig. 2), and the occurrence of upwelling over this shelf (e.g. Pickart et al., 2009, 2011). This variability and the sparseness of the data make estimates of NCP based on changes in nutrient distributions highly problematic, but it would appear that seasonal draw-down of nitrate is $\sim 5 \mu\text{M}$ over a depth of $\sim 30 \text{ m}$ (Figs. S28–S31). This yields an NCP over the vegetative season of $\sim 11 \text{ g C m}^{-2}$. This calculation does not account for upwelling events, an example of which is shown in Fig. S31. Because such events are concentrated in fall and winter (Pickart et al., 2009, 2011), it was assumed that they contribute only an additional 33% to NCP. Thus, the qualitative analysis suggests an NCP value for the southern Beaufort Sea of $\sim 15 \text{ g C m}^{-2}$. NCP values based on the data aggregated over the entire sub-re-

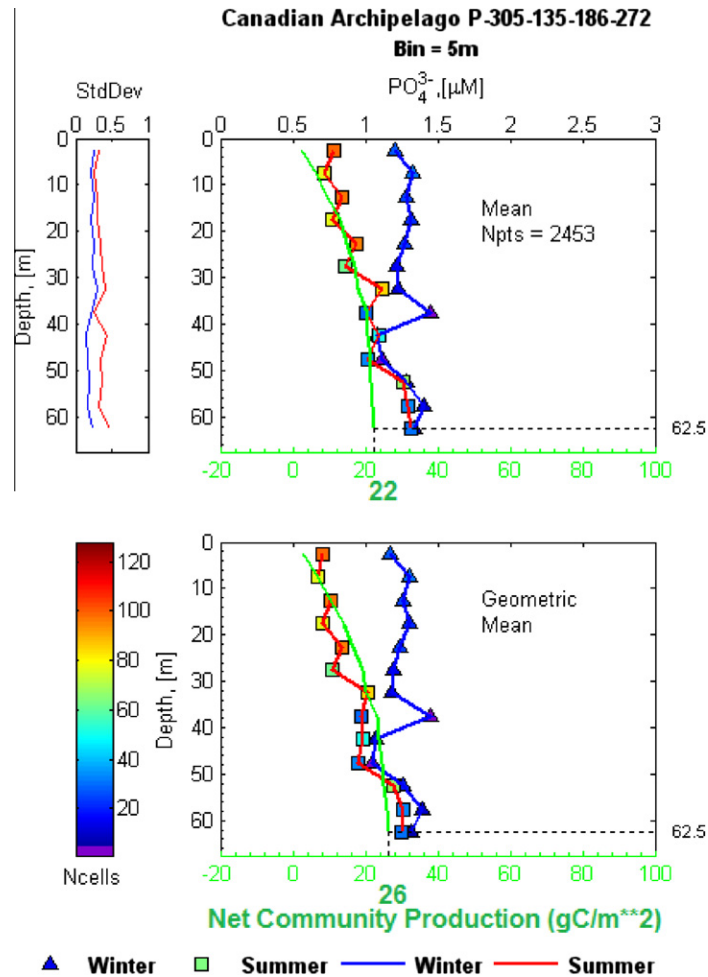


Fig. 12. Average winter (1 November–15 May) and summer (5 July–29 August) phosphate values (in μM) for the Canadian Archipelago based on data binned by 5 m depth intervals. $\text{MaxNCP-P} = 22 \text{ g C m}^{-2}$ based on the maximum integrated difference between the winter and summer arithmetic means for phosphate. Deeper integrations yielded values as high as 34 g C m^{-2} , but the deeper integrations are more likely to be aliased by water mass changes that do not reflect seasonal uptake of nutrients.

gion suggest a value of $\sim 10 \text{ g C m}^{-2}$, but the sparseness of the data and the inherent variability of this region make the computer integrations no better than the initial qualitative analysis. Only four $100 \times 100 \text{ km}$ grid squares were available for calculating maxNCP-N and for calculating maxNCP-P . The average for maxNCP-N was 7 g C m^{-2} with an SEM of $\sim 3 \text{ g C m}^{-2}$. Average maxNCP-P was 9 g C m^{-2} with an SEM of $\sim 3 \text{ g C m}^{-2}$. Lavoie et al. (2010) suggest a PP rate for the Beaufort Shelf of $\sim 25 \text{ g C m}^{-2} \text{ a}^{-1}$. We suggest an NCP value of $\sim 15 \text{ g C m}^{-2}$ for this sub-region, but it is highly speculative and the plausible range is $\sim 10\text{--}30 \text{ g C m}^{-2}$.

4.9. Kara Sea and Southern East Siberian Sea + Laptev Sub-regions

Topographic constraints, strong salt stratification and the vertical distribution of nutrients (Figs. S6, and S32–S36) suggest that net nutrient uptake in the water columns of these seas is generally restricted to the upper $\sim 20\text{--}40 \text{ m}$. River inputs impact the distribution of nutrients by intensifying stratification and by causing nutrient traps in shelf bottom waters via the two-layered estuarine counterflows that they can induce (Redfield et al., 1963; Section 2.5). Such localized nutrient traps may contribute to the phosphate maximum and associated large standard deviation in the average phosphate data from the Southern East Siberian + Laptev sub-region (Figs. S7 and S34). Our initial qualitative analysis, based on inspection of individual profiles, suggests NCPs for the Kara Sea and the Southern E. Siberian and Laptev seas of $\sim 10\text{--}20 \text{ g C m}^{-2}$. No winter data were available for these sub-regions.

Assuming pre-bloom nitrate and phosphate concentrations of 1 and $6 \mu\text{M}$ for phosphate and BigN in the Southern East Siberian Sea + Laptev sub-region and integrating over depth gave a maxNCP-P of 11 g C m^{-2} (Fig. S34) and a maxNCP-N of 8 g C m^{-2} (Fig. 13) based on BigN draw-downs. The only BigN profile from the Kara Sea is from early summer (before 20 August), and the best phosphate data also include data from early summer. Assuming initial BigN and phosphate concentrations of 6 and $0.6 \mu\text{M}$ for the Kara Sea, subtracting the average summer values and integrating over the upper $22.5\text{--}27.5 \text{ m}$ yields a BigN based NCP of 3 g C m^{-2} (Fig. S35) and a phosphate based NCP of 7 g C m^{-2} (Fig. S36). Because the data from the Kara Sea include early summer, these values are likely to be underestimates. The lack of pre-bloom data, and in the case of the Kara Sea, the lack of late summer data make these calculations extremely tenuous, and we prefer the results of our qualitative analysis. We suggest that a reasonable NCP estimate for both the Kara Sea and the Southern ESS + Laptev sub-regions is $\sim 15 \text{ g C m}^{-2}$, but the sparse data make these estimates highly uncertain. We assign a plausible range of $5\text{--}30 \text{ g C m}^{-2}$ to the estimates for these two sub-regions.

4.10. Bering Sea

As noted in Section 2.4, pre-bloom nutrient concentrations vary widely in the Bering Sea; seasonal changes in the composition of water masses in the northeastern Bering Sea can produce “apparent” NCP, and upwelling of Anadyr Water (AW) should produce

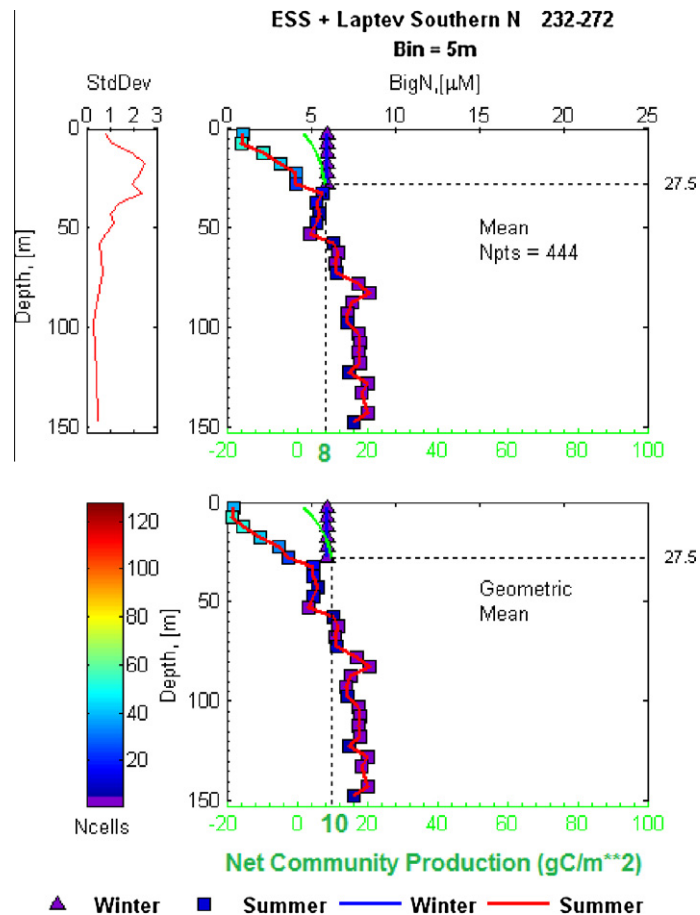


Fig. 13. Average summer (20 August–29 September) BigN values (in μM) for the East Siberian + Laptev Southern sub-region based on the maximum integrated difference between the *assumed* winter and summer arithmetic means for BigN.

Table 4

MaxNCP-N and MaxNCP-P values and standard deviations^a (in g C m^{-2}) for the 100×100 km squares for which values could be calculated.

| Region | maxNCP-N | | | maxNCP-P | | | Average ^b |
|-----------------------|----------|-----------|----------|----------------------|----------|----------|----------------------|
| | NCP | Std. dev. | <i>n</i> | NCP | Std. dev | <i>n</i> | |
| Bering Sea | 32 | 12 | 5 | 48 | 17 | 5 | 40 ^c |
| Chukchi Southern | 36 | 13 | 5 | 56 | 13 | 5 | 46 |
| Can. Archipelago | 32 | 5 | 9 | 44 | 15 | 10 | 38 |
| Barents Sea | 47 | 13 | 14 | 39 | 22 | 25 | 43 |
| Nordic Seas | 31 | 11 | 56 | 31 | 14 | 69 | 31 |
| Beaufort Southern | 7 | 5 | 4 | 9 | 6 | 4 | 8 |
| ESS + Laptev Northern | No data | | | No data | | | No data |
| Kara Sea | No data | | | No data | | | No data |
| Eurasian Basin | 13 | 11 | 6 | No data ^d | | | – |
| Chukchi Northern | No data | | | 14 | – | 2 | – |
| Greenland Shelf | 12 | 8 | 10 | 15 | 10 | 15 | 14 |
| ESS + Laptev Southern | No data | | | No data | | | No data |
| Amerasian Basin | 4 | – | 1 | No data ^d | | | No data |
| Beaufort Northern | No data | | | No data | | | No data |

^a In Section 3.9 we discuss the problems of applying routine statistics to our data. The standard deviations listed here are sample standard deviations with the number of observations (*n*) equal to the number of grid square NCP results available.

^b Average of maxNCP-N average value and maxNCP-P when both averages were available.

^c These values are likely to be significant underestimates (see Section 4.10).

^d Some maxNCP-P were available but were aliased by variations in high phosphate Pacific origin water and low phosphate Atlantic origin water (see Section 4.3).

high NCP values that would not be accounted for by $\text{NCP}_{\Delta_{\text{nut}}}$. These complications make estimation of NCP solely from seasonal changes in nutrient concentrations impossible.

The main source of nutrients is the AW that originates over the continental slope in the SW Bering Sea. This water mass rises onto the shelf and flows northward in the western Bering Sea and then into the Chukchi Sea via western Bering Strait (Hansell et al., 1989;

Sambrotto et al., 1984; Springer et al., 1989). Pre-bloom nitrate concentrations in surface layers dominated by AW can exceed $25 \mu\text{M}$ (Fig. 3). In the vicinity of western Bering Strait, stratification in AW is weak enough and turbulence strong enough to maintain high surface nutrient concentrations even during summer (Sambrotto et al., 1984; Fig. S5). In the eastern Bering Sea, low salinity ($S < \sim 31.8$) Alaska Coastal Water (ACW) has much lower

Table 5
NCP Δ_{nut} and PP by sub-region^a and AMS totals.^b

| Sub-region | NCP (m ⁻²) (g C m ⁻²) | Area (10 ¹² m ²) | NCP (Tg C) | f-ratio | PP (Tg C) |
|-----------------------|--|--|---------------|---------|--------------|
| Bering Sea | 100 (50–200) | 0.54 | 54 | 0.4 | 135 |
| Chukchi Southern | 70 (40–120) | 0.53 | 37 | 0.3 | 124 |
| Barents Sea | 40 (30–50) | 1.90 | 76 | 0.4 | 190 |
| Canadian Archipelago | 35 (20–50) | 1.33 | 47 | 0.4 | 116 |
| Nordic Seas | 30 (25–35) | 1.74 | 52 | 0.4 | 131 |
| Beaufort Southern | 15 (10–30) | 0.25 | 4 | 0.25 | 15 |
| ESS + Laptev Southern | 15 (5–30) | 0.78 | 12 | 0.25 | 47 |
| Kara Sea | 15 (5–30) | 0.86 | 13 | 0.25 | 52 |
| Eurasian Basin | 15 (5–25) | 1.45 | 22 | 0.4 | 54 |
| Greenland Shelf | 10 (5–20) | 0.76 | 11 | 0.4 | 28 |
| Chukchi Northern | 10 (5–20) | 0.65 | 6 | 0.2 | 32 |
| ESS + Laptev Northern | 8 (3–15) | 0.36 | 3 | 0.2 | 14 |
| Amerasian Basin | 3 (0.5–5) | 2.17 | 7 | 0.1 | 65 |
| Beaufort Northern | 1 (0.5–5) | 0.51 | 1 | 0.1 | 5 |
| AMS totals | – | 13.83 | 345 ± 72 | | 1008 |

^a Sub-region area includes only the portions with a marine water column.

^b The best estimate for NCP is followed by the plausible range in parentheses. The error estimate (± 72 Tg C) = the square root of the sum of the squares of the largest absolute deviations from the suggested values based on the range for each sub-region. PP = an estimate of the value that would be returned from ¹⁴C incubations.

nutrient concentrations, with pre-bloom values of $\sim 5 \mu\text{M}$ (Fig. 3). Between these extremes, Bering Shelf Water (BSW) has intermediate nutrient concentrations and salinities (Fig. 3; Springer et al., 1989; Table S1).

In and adjacent to the southwestern portion of the Bering Sea sub-region (Fig. 1b), apparent nitrate uptake exceeds $20 \mu\text{M}$ in the upper ~ 35 m, with lesser draw-downs extending to about 75 m in some cases (Fig. S37). Based on these data, we made a qualitative estimate of NCP for this region of $\sim 90 \text{ g C m}^{-2}$. Similarly, profiles from the eastern Bering Sea (Figs. 3 and S6) suggest an NCP of $\sim 8 \text{ g C m}^{-2}$. Conditions of constant upwelling of AW in the northwestern Bering Sea do not permit such calculations. Sambrotto et al. (1984) suggest that the inflow of BSW-AW functions much like a chemostat resulting in high PP whenever there is sufficient light. They suggest an annual productivity of 324 g C m^{-2} for the western Bering Strait region. With their suggested *f*-ratio of 0.55 this translates into an NCP_{bottle} of $\sim 180 \text{ g C m}^{-2}$, but this may be a minimum value because the impacts of ice algae and fall blooms were not included and the *f*-ratio may be high because of a neglect of regenerated forms of nitrogen other than ammonium. We will assume that NCP in the western Bering Strait region is $\sim 200 \text{ g C m}^{-2}$. To produce an average qualitative estimate for NCP for the Bering Sea as defined in Fig. 1b, we averaged the values for the southwest, western and eastern Bering Sea (90, 200, and 8 g C m^{-2}). This yielded a value $\sim 100 \text{ g C m}^{-2}$.

The “quantitative” estimates for this sub-region are included only for completeness. In the data aggregated by sub-region, maxNCP-N was between 24 and 41 g C m^{-2} and maxNCP-P was between 43 and 59 g C m^{-2} (Figs. S38 and S39). In the data arranged by $100 \times 100 \text{ km}$ grid squares, the average maxNCP-N was 32 g C m^{-2} and the average maxNCP-P was 48 g C m^{-2} (Table 4).

Based on our qualitative analysis we assign an average NCP value of $\sim 100 \text{ g C m}^{-2}$ to the Bering Sea sub-regions, but this value is highly uncertain and could easily range from 50 to 200 g C m^{-2} .

4.11. Southern Chukchi Sub-region

The co-occurrence and seasonal variability of ACW and higher nutrient water masses derived from AW and BSW in the southern Chukchi Sea complicate estimation of NCP from seasonal changes in nutrients. The qualitative analysis of individual profiles (Figs. S40 and S41) combined with considerations of the influence of the Anadyr Water and of upwelling in Barrow Canyon suggested an NCP of $\sim 70 \text{ g C m}^{-2}$ for the Chukchi shelf.

When aggregated over the entire sub-region, integration of the seasonal changes in BigN and phosphate yield average values for maxNCP-N and maxNCP-P of 37 and 47 g C m^{-2} , respectively (Figs. S42 and S43). The max NCP-N and maxNCP-P values from the data arranged by grid squares are sparse and suggest values of 36 and 56 g C m^{-2} , respectively, with an SEM of $\sim 6 \text{ g C m}^{-2}$ for both values. Taken at face value, these calculations suggest an NCP of $\sim 45 \text{ g C m}^{-2}$ for this sub-region. These data are likely to underestimate the influence of upwelling in Barrow Canyon and in the AW. On the other hand, advection of low nutrient ACW into the region during the warmer months may cause overestimates. Codispoti et al. (2009) suggested an NCP value between 20–80 g C m^{-2} for this region, but their calculations did not account for the possibility of upwelling in Barrow Canyon. Bates et al. (2005) suggest a range of 120–240 g C m^{-2} for NCP in the Chukchi Sea, assuming a 120 day growing season, based on seasonal changes in inorganic carbon. As noted earlier (Section 4.4), the length of their growing season is ~ 2 –3 times too long for comparison with our results, so we recalculate their estimated NCP range to be 40–120 g C m^{-2} .

Overall, the complexity of this sub-region makes estimation difficult, but we suggest that the best estimate for NCP in the Chukchi Southern sub-region is $\sim 70 \text{ g C m}^{-2}$. The correct value could plausibly lie between ~ 40 and 120 g C m^{-2} .

5. Discussion

5.1. General

A major problem for calculating NCP Δ_{nut} in most sub-regions was sparse data. In part, this was because much of the nutrient data from the Arctic is suspicious or of demonstrably poor quality. This necessitated a considerable editing effort that sometimes had to rely on experience and intuition rather than on quantitative criteria. A quote from Helland-Hansen and Nansen (1909) in their discussion of the need for high quality salinity determinations from the Norwegian Sea shows that this is not a new problem. “We have discussed this point at such length in order to urge upon future oceanographers the necessity of a very high degree of accuracy and care, if the investigations are to be of lasting value. . .”. It is a pity that more investigators have not taken this advice to heart. Included in the need for care is the proper coding of submitted data. A significant fraction of the suspicious data appeared to arise from coding and conversion errors.

The scarcity of useable pre-bloom data (\sim winter/early spring) was particularly acute. Even when data from several years were

aggregated, there was often a dearth of useable wintertime data, such that the winter and summer values that we used for our calculations may be separated by years and, in the cases of our qualitative and entire sub-region analyses, sometimes by considerable distances. Thus, estimates of NCP from several of the sub-regions required judgment, inspired by a combination of the data, previous studies, and experience. Nevertheless, we were able to arrive at a few robust conclusions, and our less robust results should help provide a base from which to launch further research. Qualitative estimates of the reliability of our NCP values for each sub-region are encapsulated in the ranges given in Table 5. This table also gives an error estimate for the AMS's total NCP.

The NCP estimate for the Nordic Seas is robust because of favorable hydrographic conditions and relatively abundant data. Although data were not abundant, hydrographic conditions in the Beaufort Northern and Amerasian Basin sub-regions mandate low NCP values, and the estimates for these regions should be correct within a few g C m^{-2} . We are also confident in asserting that the NCP regimes in the Eurasian and Amerasian Basins are significantly different with the former being more light limited and the latter more nutrient limited.

5.2. Biases

In Section 2.8 we noted that some of the biases in $\text{NCP}\Delta_{\text{nut}}$ and $\text{NCP}_{\text{bottle}}$ tend to compensate such that, in practice, the two terms may be similar although both may be low with respect to net carbon fixation. For example, we noted that our methodology for $\text{NCP}\Delta_{\text{nut}}$ does not account for nutrient regeneration below the photic zone during the vegetative season, nor does it account for excess carbon fixation after nitrate and phosphate depletion. In addition, the exact time period for maximal seasonal nutrient draw-down in any particular region is likely to \ll month. Because the time window for maximum nutrient depletion may be short and because data were so sparse in many of our sub-regions, it is likely that we have, on average, underestimated the maximum draw-down of nutrients. This would also cause our $\text{NCP}\Delta_{\text{nut}}$ estimates to be low-biased. Similarly, typical ^{14}C incubations do not determine the amount of fixation that accumulates as DOC and incubations may, in general, be low biased (e.g. Quay et al., 2010). Thus, several of the biases may cancel when we convert $\text{NCP}\Delta_{\text{nut}}$ into an estimate of PP by dividing by an appropriate f -ratio and compare these estimates with PP estimated from or keyed to typical ^{14}C incubations. It is therefore useful to note that a favorable comparison is not a sufficient condition to eliminate the possibility of low-biased results.

Nutrient concentrations were not corrected to a common salinity in part because some of the data were not accompanied by salinity values. If we assume that two meters of ice with a bulk nutrient concentration of 20% of the pre-bloom photic zone concentrations melts in summer, such melting would reduce nutrient concentrations in a 25–50 m water column by \sim 3–6%. This would cause $\text{NCP}\Delta_{\text{nut}}$ estimates to be too high by a similar amount. On the other hand, a small amount of ammonium can be present at the beginning of spring in Arctic waters (Table S1), and neglecting this “new” fixed nitrogen that may arise from sedimentary ammonium inputs would cause the NCP estimates to be too low. The combination of these two errors is likely to be small relative to other potential errors and was neglected.

5.3. $\text{NCP}\Delta_{\text{nut}}$ from maxNCP-N vs. maxNCP-P

In general, $\text{NCP}\Delta_{\text{nut}}$ estimates from maxNCP-N are similar in magnitude and correlate with estimates from maxNCP-P (Table 4; Fig. S14), but the relationship is far from perfect. In addition to errors in the data, explanations for the disparities include the follow-

ing: (1) Phosphate is not exhausted by phytoplankton uptake in AMS waters of Pacific origin, and complications arise when these waters mix with waters of Atlantic origin. Such mixing was the apparent cause of a few negative NCP values in the Eurasian and Amerasian basins, and these results were discarded (Table 4). (2) There was no requirement for the BigN and phosphate data to come from the exact same times and locations. Thus, the maxNCP-N and maxNCP-P data for a given square or sub-region, could differ in spatial and temporal distribution thereby contributing to mis-matches.

5.4. $\text{NCP}\Delta_{\text{nut}}$ vs. incubation estimates

Since $\text{NCP}\Delta_{\text{nut}}$ is similar to new production (see Section 2.8), it follows from the arguments of Eppley and Peterson (1979), that $\text{NCP}\Delta_{\text{nut}}$ should be superior to the results of ^{14}C incubations for estimating the amount of productivity that can be exported from an ecosystem. Determination of nutrient concentrations is also relatively straight forward compared to primary production incubations and the interpretation of such incubations (see Section 2.8). An advantage of $\text{NCP}\Delta_{\text{nut}}$ for computing regional rates is that the method integrates over time and, to some extent, space. On the other hand, while the characteristic of $\text{NCP}\Delta_{\text{nut}}$ of integrating over space and time is useful for determining regional rates, it is a disadvantage when attempting to understand spatial and temporal patterns, community structure, etc.

Early PP estimates may be low-biased by trace metal contamination (e.g. Fitzwater et al., 1982), and by a dearth of data from early blooms (e.g. Codispoti et al., 1991), but these problems have recently been alleviated. It is nevertheless, still difficult to properly sample and incubate samples in Arctic conditions. Given the relatively favorable conditions that exist with respect to nutrient gradients, it would, perhaps, be useful to consider a detailed comparative study of techniques somewhere within the Nordic Seas.

5.5. Conversion of $\text{NCP}\Delta_{\text{nut}}$ into PP and the total rates for each sub-region

In Sections 2.8 and 3.4 we have outlined how $\text{NCP}\Delta_{\text{nut}}$ estimates can be converted to estimates of traditional ^{14}C incubation-based PP estimates as reported in the companion paper of Hill et al. (2013). In brief, $\text{NCP}\Delta_{\text{nut}}$ (expressed as $\text{g C m}^{-2} \text{ a}^{-1}$) / f -ratio = ^{14}C PP a^{-1} . The question that arises is what is the appropriate f -ratio? Traditional studies suggest an oceanic range for this ratio of \sim 0.1–0.5 (e.g. Kanda, 1995) with the lowest values occurring in oligotrophic waters and the highest in nutrient replete productive waters (see Table 1). Wafar et al. (1996) suggest that traditional estimates are too high (by \sim 24% in polar waters) because of the neglect of urea uptake when f -ratios are calculated from the results of ^{15}N incubations. Sakshaug's (2004) review of Arctic PP (Table 1) provides values for new and total primary production. These data suggest a range of f -ratios similar to the overall oceanic range of \sim 0.1 to \sim 0.5. Within the AMS, higher f -ratios (\sim 0.65) have been found in the Northeast Water (Smith et al., 1997), in the North Water (0.58; Tremblay and Gagnon, 2009) and in western Bering Strait (Sambrotto et al., 1984). The f -ratios that exceed 0.5 represent bloom conditions and many f -ratio estimates are high biased due to the neglect of regenerated forms of nitrogen other than ammonium (e.g. urea). We will assume, therefore, that the f -ratio averaged over the vegetative season for any of our sub-regions never exceeds 0.4. We began with the data on total and new production in Table 1 and made some adjustments in order to select f -ratios for each of our sub-regions. For example, we agree with Sakshaug's (2004) ratio of \sim 0.1 for the Arctic Basin *only for that portion that is depleted in nitrate in winter* (the Amerasian and Beaufort Northern sub-regions). Because surface layer nitrate

concentrations remain appreciable in the Eurasian Basin even during summer (Figs. 4c, 9 and S2), we suggest an f -ratio of ~ 0.4 for this basin. We assumed relatively low ratios of 0.2 for the Northern ESS + Laptev Sea and Northern Chukchi sub-regions because they are influenced by low nitrate waters from the Amerasian Basin and early depletion of the low stock of nitrate should lead to greater re-cycling of nutrients. The Greenland Shelf as defined herein covers a wide range of latitudes. While it includes regions such as the Northeast Water with f -ratios above 0.5 (Smith et al., 1997), ratios are probably lower in its southern reaches and we employed an overall f -ratio of 0.3 for this sub-region. Because of constant nutrient replenishment via the AW, the western Bering Strait and Bering Sea might be expected to have an f -ratio of ~ 0.5 as suggested by Sambrotto et al. (1984), but much lower ratios would be expected in the eastern sectors due to the low nutrient content of the ACW, and a relatively long growth season. In addition, Sambrotto et al.'s (1984) estimate for western Bering Strait did not account for forms of regenerated nitrogen other than ammonium. An appropriate overall f -ratio for the Bering Sea might be about 0.4. Sakshaug's (2004) ratios of new to total production suggests an overall f -ratio for Arctic Shelf Seas of 0.25. This value is lower than some individual estimates for Arctic Seas, but we will accept it because many f -ratio estimates are high-biased. We will employ this value for the Kara Sea, Beaufort Southern, and ESS + Laptev Southern sub-regions. Because of the influence of the AW, we will assume a slightly higher ratio of 0.3 for the Chukchi Southern sub-region. Sakshaug's (2004) estimates of new and total production for the Barents Sea and Nordic Seas suggest an f -ratio of ~ 0.5 , so we have assigned our maximum value of 0.4 to these regions. He suggests a lower value for the Canadian Arctic, but his definition for this region excluded some regions of high productivity. We suggest an f -ratio of 0.4 for the Canadian Archipelago sub-region.

5.6. Perspective

Table 5 summarizes our estimates of NCP and PP by sub-region and for the entire AMS. Conversion of our NCP results to PP requires division of the NCP values by f -ratios, and choosing appropriate f -ratios introduces another potential source of error (see Section 5.5), so it is interesting that our estimate of 1008 Tg C a⁻¹ for total AMS PP was so close to the estimates of Sakshaug (2004) and Hill et al. (2013). When we normalize Sakshaug's (2004) PP estimate for the AMS to an area equal to ours, his result is 1130 Tg C a⁻¹. This is 12% higher than our estimate of 1008 Tg C a⁻¹, but Sakshaug included Hudson Bay, the Icelandic Sea, the Labrador, Sea and the Sea of Okhotsk in his estimate. Since average PP in these more southerly seas may be higher than our average, the agreement between the two estimates is surprisingly good. These results are not completely independent since we relied on Sakshaug's study for initial guidance on f -ratios, although we did not agree with him in every case.

Our result for total AMS PP also agrees well with the estimate in the companion study of Hill et al. (2013). They suggest a total PP rate for the AMS, based on ¹⁴C incubations and remote sensing data keyed to such incubations of at least 465 Tg C a⁻¹ if results are restricted to the upper portion of the photic zone where biomass was assumed to be constant, but as high as 993 Tg C a⁻¹ if PP deeper in the water column that is not captured by satellite data are included. Since there really is no reason to exclude the deeper PP, this study's estimate of 1008 Tg C a⁻¹ and their estimate of 993 Tg C a⁻¹ are quite similar (see Table 6). While the agreement between this study, Hill et al. (2013), and Sakshaug (2004) is encouraging with respect to total AMS PP, we call attention to our earlier comments about the potential for low biases in our results and in estimates keyed to typical PP incubations (see Sections

Table 6

Comparison of annual primary production (PP) values by sub-region.^a

| Sub-region | Hill et al. (Tg C a ⁻¹) | This study (Tg C a ⁻¹) | Hill et al. incl. deep PP (Tg C a ⁻¹) |
|---------------------------|--|---------------------------------------|--|
| Bering Sea | 69 | 135 | 134 |
| Chukchi Southern | 26 | 124 | 80 |
| Barents Sea | 106 | 190 | 212 |
| Canadian Archipelago | 24 | 116 | 93 |
| Nordic Seas | 162 | 131 | 308 |
| Beaufort Southern | 2 | 15 | 2 |
| ESS + Laptev Southern | 20 | 47 | 20 |
| Kara Sea | 17 | 52 | 16 |
| Greenland Shelf | 33 | 28 | 118 |
| Chukchi Northern | 1 | 32 | 6 |
| ESS + Laptev Northern | 2 | 14 | 2 |
| Arctic Basin ^b | 1 | 119 | 1 |
| Beaufort Northern | 1 | 5 | 1 |
| AMS totals ^c | 464 | 1008 | 993 |

^a Hill et al. incl. deep PP are the values adjusted for deeper PP in inflow and outflow regions (Hill et al., 2013). For comparative purposes, it is assumed that Tg C during the vegetative season \approx Tg C a⁻¹.

^b To compare our results with those of Hill et al., we have summed the values for the Eurasian and Amerasian Values (see Table 5).

^c Hill et al.'s values may slightly differ from ours (1 or 2 in the last place) due to variations in rounding.

2.8 and 5.2). We also note Sakshaug's suggestion that his estimate may be a minimum.

It is difficult to compare our values for sub-regions (Table 5) with Sakshaug's (2004) values because of differences in the way sub-regions were defined, but broadly speaking the results were similar. For example, Sakshaug gives a new production range for the East Siberian and Laptev Seas of 6–10 g C m⁻² a⁻¹. Our estimate for NCP during the vegetative season for the Northern East Siberian + Laptev sub-region is 8 g C m⁻² a⁻¹ with a plausible range of 3–15 g C m⁻². For the Southern East Siberian + Laptev sub-region, we estimate 15 g C m⁻² with a plausible range of 5–30 g C m⁻². Section 4 provides additional comparisons.

On a sub-region basis, our PP results (Table 5) did not always agree well with the results of Hill et al. (2013), and exploration of the discrepancies (Table 6) provides some useful insight. Good agreement was found for the Bering, Barents, Southern Chukchi, and Canadian Archipelago sub-regions with the ratios between estimates (higher estimate/lower estimate) ranging from 1.01 to 1.55. These regions are productive and account for 52% of the AMS total in Hill et al. (2013) and 56% of the total AMS PP estimated in this study.

The largest relative differences occurred in sub-regions (ESS + Laptev Northern, Southern Beaufort, Northern Beaufort, Northern Chukchi, and Arctic Basin) with heaviest ice-cover. The lower values obtained by Hill et al. (2013) for these regions may arise because their algorithms assumed no productivity when ice-cover was greater than 40%. As they noted, this approach excludes production by ice algae and production under the ice which can be significant in these regions once the snow cover on the ice has melted (see discussion in Hill et al. (2013)). These are all regions with relatively low productivity. Setting aside the Arctic Basin sub-region for the moment, the ratios, between high and low estimates ranged between 5.00 and 7.50. These sub-regions accounted for only 1% of Hill et al.'s total estimate, and 7% of this study's total, so the large relative differences between estimates did not greatly impact the total.

The Arctic Basin sub-region in Table 6 includes the productivity in the Eurasian and Amerasian Basin sub-regions (Table 5). Here we find the worst relative comparison between our study and Hill et al. (2013), and also a large absolute difference.

The ratio between the high and low estimates for the Arctic Basin was 119 (Table 6), and the absolute difference between the two

estimates was 118 Tg C a^{-1} . Average productivity was relatively low in both studies, but the region is vast and accounted for 12% of total AMS PP in our estimate while making only a negligible contribution to the estimate of Hill et al. (2013). Since much of the productivity in this region is ice-associated (e.g. Gosselin et al., 1997), the failure to account for such productivity in the algorithms of Hill et al. may explain the difference as these authors have noted. We chose a low f -ratio of 0.1 for the Amerasian Basin that might also contribute to the difference. Finally, lumping the moderately productive Eurasian Basin with the oligotrophic Amerasian Basin could alias Hill et al.'s results if there is an uneven distribution of data between the two sub-basins.

There was a major difference between our PP estimate for the Nordic Seas of 131 Tg C a^{-1} and Hill et al.'s (2013) estimate of 308 Tg C^{-1} . The relatively deep MLDs that occur in this region could contribute to this difference. Mixing events that contribute to the deep MLDs may transport organic material below the photic zone leading to nutrient regeneration during the vegetative season that can suppress our estimates of NCP, and it is possible that our choice of an f -ratio for this region was too high. We can only speculate at this point that the true value lies between the two estimates.

Our PP estimate of 28 Tg C a^{-1} for the Greenland Shelf sub-region was only about one fourth of Hill et al.'s (2013) estimate of 118 Tg C a^{-1} . Broadly speaking there is likely to be a strong cross-shelf gradient in PP in this sub-region with heavier ice-cover towards the coast, and the offshore boundary grading into conditions more typical of the abutting higher productivity Nordic Seas and Canadian Archipelago sub-regions. Since it is possible that the distribution of remote sensing and in situ productivity estimates were weighted towards the offshore boundaries and to productive polynyas, it is possible that spatial aliasing in these data introduce a high-bias. Once again, we suggest that the true value may lie between our estimate and the estimate of Hill et al.

We have already noted that our NCP estimates for the Kara Sea and Southern ESS + Laptev sub-regions suffer from extremely sparse data (Section 4.9), so it is not surprising that the combined PP values for these regions differ significantly with this study estimating PP at 99 Tg C a^{-1} and Hill et al. (2013) estimating 36 Tg C a^{-1} .

5.7. Change

The AMS is highly variable. This system is sensitive to global change and the pace of change has accelerated to include drastic decreases in ice cover in recent years (Serreze et al., 2009). With respect to inter-annual change, it has already been noted that PP in the Barents Sea tends to be higher during warmer years (Carmack et al., 2006). In recent years significant hydrographic changes with a \sim decadal time scale have also been documented (e.g. Steele and Boyd, 1998). There is a consensus that the overall trajectory is for decreased ice cover and increased warming.

Unfortunately, the sparse data made it problematic to investigate temporal variability in NCP. Overall, it is more difficult to estimate the trajectory of NCP than PP's trajectory because PP includes a re-cycled component that can respond to an increased photon flux and to increased temperature without requiring additional nutrients. For example, comparison of data from the Chukchi Shelf collected in 2002 and 2004 suggested higher PP during the warmer year (2004), but how this would translate into changes in NCP during the vegetative season was uncertain. This was because the nutrient pool was probably higher during 2002, and the 2002 observations may not have captured the end of the vegetative season (Codispoti et al., 2009).

Temperature regulates phytoplankton physiology in temperate waters (Eppley, 1972), and increased temperature is likely to cause modest increases of total PP and respiration even over the relatively restricted range of AMS temperatures (e.g. Kirchner et al.,

2009). Increases in the availability of light with decreased ice cover in the AMS have been suggested as raising the possibility of large increases in PP in the future (e.g. Arrigo et al., 2008). Because fixed-N is stripped from much of the surface layer during summer (e.g. Fig. 4a–c), the impact of increased temperature and light on PP may be damped without an increased nutrient supply, but the overall trajectory is likely to be positive.

Since the AMS's nutrient supply is heavily utilized under present-day conditions (Fig. 4a–c) and since NCP, new production and export production depend critically on the nutrient supply, the trajectory of these types of productivity will be highly dependent on changes in the nutrient supply. We can posit plausible scenarios for increases or decreases in the nutrient supply. For example, decreased ice cover should cause increased vertical mixing that might enhance the nutrient supply, but an increase in river flow (Lavoie et al., 2010; Tremblay and Gagnon, 2009) would tend to increase stratification and could reduce inputs of nutrients into the photic zone. Plausible changes in the advective inputs of nutrients could also be positive or negative (e.g. an increase or decrease in the AW inflow). In addition, light penetration could decrease in some regions due to increased riverine inputs of particulate matter and colored dissolved matter, as well as increased wind mixing in shallow seas (e.g. Forest et al., 2008). Finally, as suggested by Measures (1999), reduction in ice cover might increase the importance of iron limitation. It is also worth noting that decreases in export production from the photic zone may arise from a reduction in the size of phytoplankton as the surface layers of the Arctic freshen (Li et al., 2009).

Overall, the extant studies and the characteristics of the AMS suggest that predictions of several-fold increases in PP in the next \sim 50 years are not likely, but moderate increases are plausible. Changes in NCP are harder to predict, and, to date, there is no compelling evidence to suggest whether the trajectory of NCP will be positive or negative.

6. Concluding comments and cautionary notes

Robust conclusions from this analysis include the seasonal changes in nutrient values for the Nordic Seas where there were relatively abundant high quality data, plus a hydrographic set-up that favors calculation of NCP from changes in nutrient concentrations. Conditions for the Barents Sea calculations, although not as favorable, also gave us some confidence in the quantitative estimates for this sub-region. The low wintertime nitrate concentrations in the Northern Beaufort Sea and adjacent Amerasian Basin would seem to be a sufficient condition to allow one to assert that NCP in this region is quite low and not likely to change much unless nitrate from depths of \sim 50 m and greater can be made available for phytoplankton growth. We have also been able to demonstrate geographic differences in controls and rates of NCP between the Amerasian and Eurasian Basins. This study also supports previous results that suggest that the differences in PP and NCP between AMS sub-regions range over two orders of magnitude (Tables 1, 5 and 6). It is also possible that the edited phosphate, nitrate and BigN data employed in this study might prove superior for model validation since many highly suspicious values occurred in some existing data bases.

While the sparse data (particularly pre-bloom data) added considerable uncertainty to some of our estimates, the results were encouraging enough to suggest that an increase of high-quality time-series nitrate data from the AMS would enable calculation of NCP values in some of our sub-regions that might be highly useful for estimating export production and that would be free of some of the complications associated with incubation techniques. Given the problems with incubation-based estimates of PP and the importance of NCP as a variable that sets an upper limit on

export production, we suggest that an increased emphasis on obtaining high quality nutrient time-series from the Arctic would be useful. This is increasingly feasible because of the recent development of autonomous sensors for nitrate and other nutrients (Glibert et al., 2008; Johnson et al., 2010).

Although the agreement of our overall estimate for Arctic Ocean PP with other estimates is encouraging, the reader is cautioned to view this analysis as a starting point rather than a last word. The relatively good agreement on overall PP could be fortuitous given the uncertainties arising from sparse data, the need for subjective data editing in some cases, the reliance on qualitative analysis for several sub-regions, etc. In addition to convert our NCP estimates to PP, we had to rely on literature estimates of f -ratios (see Section 5.5). Some of our f -ratio estimates were based on estimates of total and new production in Sakshaug (2004), and we compare our estimate for total AMS PP with his. Thus, it could be argued that there is a degree of circularity in this particular comparison, even though we do not totally agree with the f -ratios suggested by Sakshaug's analysis, and even though our NCP estimates were independent. Finally, because the Arctic is changing, even a highly accurate estimate for past productivity might not apply to the future. Much more needs to be done, and, as we have suggested, this includes obtaining improved time-series for nutrient concentrations.

Acknowledgements

The senior author (LAC) gratefully acknowledges support for his Arctic research from the Office of Naval Research and the National Science Foundation that began with an expedition on the USCGC Northwind in 1963. This contribution was funded by a suite of awards to the authors under the aegis of the National Science Foundation's Arctic System Science's synthesis initiative. The senior author also acknowledges salary support from the University of Maryland's Center for Environmental Sciences during the initial stages of this effort. We are also grateful to L.S. Codispoti for proof-reading this manuscript and to Deborah C. Hinkle for her careful calculations and data entry. We thank R. Key, K. Falkner, and F. McLaughlin for providing important data and V. Coles and J. Marra for helpful comments.

The developers of Ocean Data View (Schlitzer, 2007) are gratefully acknowledged for making this outstanding data plotting and analysis tool available free of charge to academia. We also thank the five reviewers who took the time to read and comment on this lengthy contribution. Many of their comments were very helpful.

Finally, we thank those intrepid and responsible investigators who made good quality data available and those data managers who properly entered the data into public domain data bases.

Appendix A. Supplementary material

The supplementary data, figures and tables associated with this article can be found in the online version, at <http://dx.doi.org/10.1016/j.pocean.2012.11.006>.

References

Aagaard, K., 1984. The Beaufort undercurrent. In: Barnes, P.W., Schell, D.M., Reimnitz, E. (Eds.), *The Alaskan Beaufort Sea: Ecosystems and Environments*. Academic Press, San Diego, pp. 47–72.

Aguilar-Islas, A.M., Hurst, M.P., Buck, K.N., Sohst, B., Smith, G.J., Lohan, M.C., Bruland, K.W., 2007. Micro- and macronutrients in the southeastern Bering Sea: insight into iron-replete and iron-depleted regimes. *Progress in Oceanography* 73, 99–126.

Anderson, L.A., 1995. On the hydrogen and oxygen content of marine phytoplankton. *Deep-Sea Research* 42, 1675–1680.

Anderson, L.A., Sarmiento, J.L., 1994. Redfield ratios of remineralization determined by nutrient data analysis. *Global Biogeochemical Cycles* 8, 65–80.

Antonov, V.S., 1957. The principal causes of fluctuations in ice conditions of the Arctic seas. *Problemi Arktiki* 1, 41–50 (Translation).

Arrigo, K.R., Dijken, G.V., Pableni, S., <http://dx.doi.org/10.1029/2008GL035028>, 2008. Impact of a shrinking Arctic ice cover on marine primary production. *Geophysical Research Letters* 35.

Baines, S.B., Pace, M.L., 1991. The production of dissolved organic matter by phytoplankton and its importance to bacteria. *Limnology and Oceanography* 36, 1078–1090.

Bates, N.R., Best, M.H.P., Hansell, D.A., 2005. Spatio-temporal distribution of dissolved inorganic carbon and net community production in the Chukchi and Beaufort Seas. *Deep-Sea Research II* 52, 3303–3323.

Berger, W.H., 1970. Biogenous deep-sea sediments: fractionation by deep-sea circulation. *Geological Society of America Bulletin* 81, 1385–1402.

Broecker, W.S., 1991. The great ocean conveyor. *Oceanography* 4, 79–89.

Carmack, E.C., 2007. The alpha/beta ocean distinction: a perspective on freshwater fluxes, convection, nutrients and productivity in high-latitude seas. *Deep-Sea Research II* 54, 2578–2598.

Carmack, E.C., Macdonald, R.W., 2001. Oceanography of the Canadian Shelf of the Beaufort Sea: a setting for marine life. *Arctic* 55, 29–45.

Carmack, E., Barber, D., Christensen, J., Macdonald, R., Rudels, B., Sakshaug, E., 2006. Climate variability and physical forcing of the food webs and the carbon budget on panarctic shelves. *Progress in Oceanography* 71, 145–181.

Carpenter, E.J., Romans, K., 1991. Major role of the cyanobacterium *Trichodesmium* in nutrient cycling in the North Atlantic. *Science* 254, 1356–1358.

Codispoti, L.A., Owens, T.G., 1975. Nutrient transports through Lancaster Sound in relation to the Arctic Ocean's reactive silicate budget and the outflow of Bering Strait waters. *Limnology and Oceanography* 20, 115–119.

Codispoti, L.A., Richards, F.A., 1968. Micronutrient distributions in the East Siberian and Laptev seas during summer 1963. *Arctic* 21, 67–85.

Codispoti, L.A., Friederich, G.E., Sakamoto, C.M., Gordon, L.I., 1991. Nutrient cycling and primary production in the marine systems of the Arctic and Antarctic. *Journal of Marine Systems* 2, 359–384.

Codispoti, L.A., Flagg, C., Kelly, V., Swift, J.H., 2005. Hydrographic conditions during the 2002 SBI process experiments. *Deep-Sea Research II* 52, 3199–3226.

Codispoti, L.A., Flagg, C., Swift, J.H., 2009. Hydrographic conditions during the 2004 SBI process experiments. *Deep-Sea Research II* 56, 1144–1163.

Colony, R., Timokhov, L., 2001. *Hydrochemical Atlas of the Arctic Ocean*. International Arctic Research Center, University of Alaska, USA & State Research Center—the Arctic and Antarctic Research Institute, Russia, CD-ROM.

Cooper, L.W., Codispoti, L.A., Kelly, V., Sheffield, G.G., Grebmeier, J.M., 2006. The potential for using Little Diomedede Island as a platform for observing environmental conditions in Bering Strait. *Arctic* 59, 129–141.

Dugdale, R.C., Goering, J.J., 1967. Uptake of new and regenerated forms of nitrogen in primary production. *Limnology and Oceanography* 12, 196–206.

Eppley, R.W., 1972. Temperature and phytoplankton growth in the sea. *Fishery Bulletin* 70, 1063–1085.

Eppley, R.W., Peterson, B.J., 1979. Particulate organic matter flux and planktonic new production in the deep ocean. *Nature* 282, 677–680.

Fitzwater, S.E., Knauer, G.A., Martin, J.H., 1982. Metal contamination and its effect on primary production measurements. *Limnology and Oceanography* 27, 544–551.

Forest, A., Sampei, M., Makabe, R., Sasaki, H., Barber, D.G., Gratton, Y., Wassman, P., Fortier, L., <http://dx.doi.org/10.1029/2007JC004262>, 2008. The annual cycle of particulate organic carbon in Franklin Bay (Canadian Arctic): environmental control and food web implications. *Journal of Geophysical Research* 113, C03S0r.

Glibert, P.M., Kelly, V., Alexander, J., Codispoti, L.A., Boicourt, W.C., Trice, M.T., Michael, B., 2008. *In situ* nutrient monitoring: a tool for capturing nutrient variability and the antecedent conditions that support algal blooms. *Harmful Algae* 8, 175–181.

Gordeev, V.V., 2000. River input of water, sediment, major ions, nutrients and trace metals from Russian territory to the Arctic Ocean. In: Lewis, E.L., Jones, E.P., Lemke, P., Prowse, T.D., Wadhams, P. (Eds.), *The Freshwater Budget of the Arctic Ocean*. Kluwer Academic Publishers, Dordrecht, pp. 297–322.

Gordeev, V.V., Martin, J.M., Sidorov, I.S., Sidorova, M.V., 1996. A reassessment of the Eurasian river input of water, sediment, major elements, and nutrients to the Arctic Ocean. *American Journal of Science* 296, 664–691.

Gordon, A., 1986. Inter-ocean exchange of thermocline water. *Journal of Geophysical Research* 91, 5037–5046.

Gosselin, M., Levasseur, M., Wheeler, P.A., Horner, R.A., Booth, B.C., 1997. New measurements of phytoplankton and ice algal production in the Arctic Ocean. *Deep-Sea Research II* 44, 1623–1644.

Hansell, D.A., Goering, J.J., Walsh, J.J., McRoy, C.P., Coachman, L.K., Whitedge, T.E., 1989. Summer phytoplankton production and transport along the shelf break in the Bering Sea. *Continental Shelf Research* 9, 1085–1104.

Helland-Hansen, B., Nansen, F., 1909. The Norwegian Sea: its physical oceanography based upon the Norwegian researches 1900–1904. *Norwegian Fishery and Marine-Investigations* 11, 1–360.

Hill, V.J., <http://dx.doi.org/10.1029/2007JC004119>, 2008. Impacts of chromophoric dissolved organic material on surface ocean heating in the Chukchi Sea. *Journal of Geophysical Research* 113, C07024.

Hill, V.J., Cota, G., 2005. Spatial patterns of primary production on the shelf, slope and basin of the Western Arctic in 2002. *Deep-Sea Research II* 52, 3344–3354.

Hill, V.J., Zimmerman, R., <http://dx.doi.org/10.1016/j.dsr.2010.06.011>, 2010. Estimates of primary production by remote sensing in the Arctic Ocean: assessment of accuracy with passive and active sensors. *Deep-Sea Research I* 57, 1243–1254.

- Hill, V.J., Matrai, P., Olson, E., Suttles, S., Steele, M., Codispoti, L.A., Zimmerman, R., <http://dx.doi.org/10.1016/j.pocean.2012.11.005>, 2013. Synthesis of integrated primary production in the Arctic Ocean: II. *In situ* and remotely integrated estimates. *Progress in Oceanography* 110, 107–125.
- Hoppema, M., Goeyens, L., 1999. Redfield behavior of carbon, nitrogen and phosphorus depletions in Antarctic surface water. *Limnology and Oceanography* 44, 220–224.
- Jackson, G.A., 1993. The importance of the DOC pool for primary production estimates. *ICES Marine Sciences Symposium* 197, 141–148.
- Johnson, K.S., Riser, S.C., Karl, D.M., 2010. Nitrate supply from deep to near-surface waters of the North Pacific subtropical gyre. *Nature* 465, 1062–1065.
- Jones, B.M., Arp, C.D., Jorgenson, M.T., Hinkel, K.M., Schmutz, J.A., Flint, P.L., <http://dx.doi.org/10.1029/2008GL036205>, 2009. Increase in the rate and uniformity of coastline erosion in Arctic Alaska. *Geophysical Research Letters* 36, L03503.
- Kähler, P., Koeve, W., 2001. Marine dissolved organic matter: can its C:N ratio explain carbon overconsumption? *Deep-Sea Research I* 48, 49–62.
- Kanda, J., 1995. Nitrate assimilation and new production in open ocean. In: Sakai, H., Nozaki, Y. (Eds.), *Biogeochemical Processes and Ocean Flux in the Western Pacific*. Terra Scientific Publishing Company, Tokyo, pp. 227–238.
- Kattner, G., Budéus, G., 1997. Nutrient status of the Northeast Water Polynya. *Journal of Marine Systems* 10, 185–197.
- Kirchman, D.L., Hill, V., Cottrell, M.T., Gradinger, R., Malmstrom, R.R., Parker, A., 2009. Standing stocks, production, and respiration of phytoplankton and heterotrophic bacteria in the western Arctic Ocean. *Deep-Sea Research II* 56, 1237–1248.
- Koeve, W., 2004. Spring bloom carbon to nitrogen ratio of net community production in the temperate N Atlantic. *Deep-Sea Research I* 51, 1579–1600.
- Lavoie, D., Denman, L.K., Macdonald, R.W., <http://dx.doi.org/10.1029/2009JCO05493>, 2010. Effects of future climate change on primary productivity and export fluxes in the Beaufort Sea. *Journal of Geophysical Research* 115, C04018.
- Le Bouteiller, A., 1993. Comparison of in-bottle measurements using ^{15}N and ^{14}C . *ICES Marine Sciences Symposium* 197, 121–133.
- Legendre, L., Gosselin, M., 1989. New production and export of organic matter to the deep ocean: consequences of some recent discoveries. *Limnology and Oceanography* 34, 1374–1380.
- Li, W.K.W., McLaughlin, F.A., Lovejoy, C., Carmack, E.C., 2009. Smallest algae thrive as the Arctic Ocean Freshens. *Science* 326, 539.
- Macdonald, R.W., Sakshaug, E., Stein, R., 2004. The Arctic Ocean: modern status and recent climate change. In: Stein, R., Macdonald, R.W. (Eds.), *The Organic Carbon Cycle in the Arctic Ocean*. Springer, Berlin, pp. 297–322.
- Mague, T.H., Friberg, E., Hughes, D.J., Morris, I., 1980. Extracellular release of carbon by marine phytoplankton. *Limnology and Oceanography* 25, 262–279.
- Marra, J., 2009. Net and gross productivity: weighing in with ^{14}C . *Aquatic Microbial Ecology* 56, 123–131.
- Mathis, J.T., Bates, N.R., Hansell, D.A., Babila, T., 2009. Net community production in the northeastern Chukchi Sea. *Deep-Sea Research II* 56, 1213–1222.
- Matrai, P.A., Olson, E., Suttles, S., Hill, V., Codispoti, L.A., Light, B., Steele, M., 2012. Synthesis of primary production in the Arctic Ocean I. Surface waters, 1954–2007. *Progress in Oceanography*
- Measures, C.I., 1999. The role of entrained sediments in sea ice in the distribution of aluminium and iron in the surface waters of the Arctic Ocean. *Marine Chemistry* 68, 59–70.
- Olli, K., Wassmann, P., Reigstad, M., Ratkova, T.N., Arashkevich, E., Pasternak, A., Matrai, P.A., Knulst, J., Tranvik, L., Klais, R., Jacobsen, A., 2007. The fate of production in the central Arctic Ocean – top-down regulation by zooplankton expatriates? *Progress in Oceanography* 72, 84–113.
- Östlund, H.G., 1982. The residence time of the freshwater component in the Arctic Ocean. *Journal of Geophysical Research* 87, 2035–2043.
- Packard, T.T., Codispoti, L.A., 2007. Respiration, mineralization, and biochemical properties of the particulate matter in the Nansen basin water column in April 1981. *Deep-Sea Research I* 54, 403–414.
- Peterson, B.J., 1980. Aquatic primary productivity and the ^{14}C - CO_2 method: a history of the productivity problem. *Annual Review of Ecology and Systematics* 11, 359–385.
- Peterson, B.J., Holmes, R.M., McClelland, J.W., Vörösmarty, C.J., Lammers, R.B., Shiklomanov, A.I., Shiklomanov, I.A., Rahmstorf, S., 2002. Increasing river discharge to the Arctic Ocean. *Science* 298, 2171–2173.
- Piatt, J.F., Springer, A.M., 2003. Advection, pelagic food webs and the biogeography of seabirds in Beringia. *Marine Ornithology* 31, 141–154.
- Pickart, R.S., Moore, G.W.K., Torres, D.J., Fratantoni, P., Goldsmith, R.A., Yang, J., <http://dx.doi.org/10.1029/2208JC005009>, 2009. Upwelling on the continental slope of the Alaskan Beaufort Sea; Storms, ice and oceanographic response. *Journal of Geophysical Research* 114, C00A13.
- Pickart, R.S., Spall, M.A., Moore, G.W.K., Weingartner, T.J., Woodgate, R.A., Aagaard, K., Shimada, K., <http://dx.doi.org/10.1016/j.pocean.2010.11.005>, 2011. Upwelling in the Alaskan Beaufort Sea: atmospheric forcing and local versus non-local response. *Progress in Oceanography* 88, 78–100.
- Quay, P.D., Peacock, C., Björkman, K., Karl, D.M., <http://dx.doi.org/10.1029/2009GB003665>, 2010. Measuring primary production rates in the ocean: Enigmatic results between incubation and non-incubation methods at Station ALOHA. *Global Biogeochemical Cycles* 24, GB3014.
- Redfield, A., Ketchum, B.H., Richards, F.A., 1963. The influence of organisms on the composition of seawater. In: Hill, M.N. (Ed.), *The Sea*. Academic Press, New York, pp. 26–77.
- Robinson, C., Williams, P.J.leB., 2005. Respiration and its measurement in surface marine waters. In: delGiorgio, P., Williams, P.J.leB. (Eds.), *Respiration in Aquatic Ecosystems*. Oxford University Press, New York, pp. 147–180.
- Sakshaug, E., 1997. Biomass and productivity distributions and their variability in the Barents Sea. *ICES Journal of Marine Science* 54, 350–431.
- Sakshaug, E., 2004. Primary and secondary production in the Arctic seas. In: Stein, R., Macdonald, R.W. (Eds.), *The Organic Carbon Cycle in the Arctic Ocean*. Springer-Verlag, Berlin, pp. 57–81.
- Sakshaug, E., Slagstad, D., 1992. Sea-ice and wind effects on primary productivity in the Barents Sea. *Atmosphere-Ocean* 30, 579–591.
- Sambrotto, R.N., Goering, J.J., McRoy, C.P., 1984. Large yearly production of phytoplankton in the western Bering Strait. *Science* 225, 161–198.
- Sambrotto, R.N., Savidge, G., Robinson, C., Boyd, P., Takahashi, T., Karl, D.M., Langdon, C., Chipman, D., Marra, J., Codispoti, L.A., 1993. Net organic carbon production of marine plankton exceeds estimates based on nitrate limitation. *Nature* 363, 248–250.
- Schlitzer, R., 2007. Ocean Data View. <<http://odv.awi.de>>.
- Serreze, M.C., Barrett, A.P., Stroeve, J.C., Kindig, D.N., Holland, M.M., 2009. The emergence of surface-based Arctic amplification. *The Cryosphere* 3, 11–19.
- Sintes, E., Stoderegger, K., Parada, V., Herndl, G.J., 2010. Seasonal dynamics of dissolved organic matter and microbial activity in the coastal North Sea. *Aquatic Microbial Ecology* 60, 85–95.
- Smith, W.O., Niebauer, H.J., 1993. Interactions between biological and physical processes in Arctic seas: investigations using numerical models. *Reviews of Geophysics* 31, 189–209.
- Smith, W.O., Codispoti, L.A., Nelson, D.M., Manley, T., Buskey, E.J., Niebauer, H.J., Cota, G.F., 1991. Importance of *Phaeocystis* blooms in the high-latitude ocean carbon cycle. *Nature* 352, 514–516.
- Smith, W., Gosselin, M., Legendre, L., Wallace, D., Daly, K., Kattner, G., 1997. New production in the Northeast Water Polynya: 1993. *Journal of Marine Systems* 10, 199–209.
- Springer, A.M., McRoy, C.P., Turco, K.R., 1989. The paradox of pelagic food webs in the northern Bering Sea – II. Zooplankton communities. *Continental Shelf Research* 9, 359–386.
- Stabeno, P.J., Hunt, G.L., Napp, J.M., Schumacher, J.D., 2005. Physical forcing of ecosystem dynamics on the Bering Sea shelf. In: Robinson, A.R., Brink, K. (Eds.), *The Sea*, vol. 14. Harvard University Press, pp. 1177–1212.
- Steele, M., Boyd, T., 1998. Retreat of the cold halocline layer in the Arctic Ocean. *Journal of Geophysical Research* 103, 10419–10435.
- Stein, R., Macdonald, R.W., 2004. *The Organic Carbon Cycle in the Arctic Ocean*. Springer-Verlag, Berlin, 363 pp.
- Stirling, I., 1980. The biological importance of polynyas in the Canadian Arctic. *Arctic* 33, 303–315.
- Tremblay, J.-E., Gagnon, J., 2009. The effects of irradiance and nutrient supply on the productivity of Arctic waters: a perspective on climate change. In: Nihoul, J.C.J., Kostianoy, A.G. (Eds.), *Influence of Climate Change on the Changing Arctic and Sub-Arctic Conditions*. Springer, Dordrecht, pp. 73–92 (NATO Science Series).
- Tremblay, J.-E., Gratton, Y., Fauchot, J., Price, N., 2002. Climatic and oceanic forcing of new, net and diatom production in the North Water. *Deep-Sea Research II* 49, 4926–4927.
- Vernet, M., Matrai, P.A., Andeassen, I., 1998. Synthesis of particulate and extracellular carbon by phytoplankton at the marginal ice zone in the Barents Sea. *Journal of Geophysical Research* 103, 1023–1037.
- Wafar, M.V., Le Corre, P., L'Helguen, S., 1996. F-ratios calculated with and without urea in nitrogen uptake by phytoplankton. *Deep-Sea Research I* 42, 1669–1674.
- Wassmann, P., Reigstad, M., 2011. Future Arctic Ocean seasonal ice zones and implications for pelagic–benthic coupling. *Oceanography* 24, 220–231.
- Wheeler, P.A., 1997. Preface: the 1994 Arctic Ocean section. *Deep-Sea Research II* 44, 1483–1485.
- Williams, P.J.leB., 1993a. On the definition of plankton production terms. *ICES Marine Sciences Symposium* 197, 9–19.
- Williams, P.J.leB., 1993b. Chemical and tracer methods of measuring plankton production. *ICES Marine Sciences Symposium* 197, 20–36.
- Woodgate, R.A., Aagaard, K., <http://dx.doi.org/10.1029/2004GL021747>, 2005. Revising the Bering Strait freshwater flux into the Arctic Ocean. *Geophysical Research Letters* 32, L02602.
- Woodgate, R.A., Aagaard, K., Weingartner, T.J., <http://dx.doi.org/10.1029/2006GL026931>, 2006. Interannual changes in the Bering Strait fluxes of volume, heat and freshwater between 1991 and 2004. *Geophysical Research Letters* 33, L15609.
- Zhang, J., Rothrock, D., Steele, M., 2000. Recent changes in Arctic sea ice: the interplay between ice dynamics and thermodynamics. *Journal of Climate* 13, 3099–3114.
- Zheng, Y., Schlosser, P., Swift, J.W., Jones, E.P., 1997. Oxygen utilization rates in the Nansen Basin, Arctic Ocean: implications for new production. *Deep-Sea Research I* 44, 1923–1943.